POLITECNICO
MILANO 1863

Department of
Electronics, Informatics and Bioengineering
M.Sc. course of Computer Science and Engineering

Adversarially Learned Anomaly Detection Using Generative Adversarial Networks

Supervisor:
Doc. Giacamo Boracchi — Politecnico di Milano

Master of Science Thesis of:
Şemsi Yiğit Özgümüş
Matriculation ID 893558

July 2019

Abstract

Lorem ipsum dolor sit amet, consectetuer adipiscing elit. Ut purus elit, vestibulum ut, placerat ac, adipiscing vitae, felis. Curabitur dictum gravida mauris. Nam arcu libero, nonummy eget, consectetuer id, vulputate a, magna. Donec vehicula augue eu neque. Pellentesque habitant morbi tristique senectus et netus et malesuada fames ac turpis egestas. Mauris ut leo. Cras viverra metus rhoncus sem. Nulla et lectus vestibulum urna fringilla ultrices. Phasellus eu tellus sit amet tortor gravida placerat. Integer sapien est, iaculis in, pretium quis, viverra ac, nunc. Praesent eget sem vel leo ultrices bibendum. Aenean faucibus. Morbi dolor nulla, malesuada eu, pulvinar at, mollis ac, nulla. Curabitur auctor semper nulla. Donec varius orci eget risus. Duis nibh mi, congue eu, accumsan eleifend, sagittis quis, diam. Duis eget orci sit amet orci dignissim rutrum.

Sommario

Lorem ipsum dolor sit amet, consectetuer adipiscing elit. Ut purus elit, vestibulum ut, placerat ac, adipiscing vitae, felis. Curabitur dictum gravida mauris. Nam arcu libero, nonummy eget, consectetuer id, vulputate a, magna. Donec vehicula augue eu neque. Pellentesque habitant morbi tristique senectus et netus et malesuada fames ac turpis egestas. Mauris ut leo. Cras viverra metus rhoncus sem. Nulla et lectus vestibulum urna fringilla ultrices. Phasellus eu tellus sit amet tortor gravida placerat. Integer sapien est, iaculis in, pretium quis, viverra ac, nunc. Praesent eget sem vel leo ultrices bibendum. Aenean faucibus. Morbi dolor nulla, malesuada eu, pulvinar at, mollis ac, nulla. Curabitur auctor semper nulla. Donec varius orci eget risus. Duis nibh mi, congue eu, accumsan eleifend, sagittis quis, diam. Duis eget orci sit amet orci dignissim rutrum.

Acknowledgements

Lorem ipsum dolor sit amet, consectetuer adipiscing elit. Ut purus elit, vestibulum ut, placerat ac, adipiscing vitae, felis. Curabitur dictum gravida mauris. Nam arcu libero, nonummy eget, consectetuer id, vulputate a, magna. Donec vehicula augue eu neque. Pellentesque habitant morbi tristique senectus et netus et malesuada fames ac turpis egestas. Mauris ut leo. Cras viverra metus rhoncus sem. Nulla et lectus vestibulum urna fringilla ultrices. Phasellus eu tellus sit amet tortor gravida placerat. Integer sapien est, iaculis in, pretium quis, viverra ac, nunc. Praesent eget sem vel leo ultrices bibendum. Aenean faucibus. Morbi dolor nulla, malesuada eu, pulvinar at, mollis ac, nulla. Curabitur auctor semper nulla. Donec varius orci eget risus. Duis nibh mi, congue eu, accumsan eleifend, sagittis quis, diam. Duis eget orci sit amet orci dignissim rutrum.

Contents

Abstract iii

Sommario v

Acknowledgements vii

Contents viii

List of Figures x

List of Tables xi

1 Introduction 1

2 State of the Art 3
2.1 Anomaly Detection . . . 3
2.1.1 Related Works . . . 7
2.2 Architectural Components . . . 8
2.2.1 Generative Adversarial Networks . . . 8
2.2.2 Autoencoder Networks . . . 14
2.3 GAN Based Anomaly Detection Methods . . . 17
2.3.1 AnoGAN . . . 18
2.3.2 BiGAN and ALI . . . 20
2.3.3 ALAD . . . 27
2.3.3.1 Spectral Normalization . . . 27
2.3.3.2 Conditional Entropy (ALICE Framework) . . . 28
2.3.3.3 ALAD Architecture . . . 30
2.3.4 GANomaly & Skip-GANomaly . . . 33

3 Latest Developments 37
3.1 F-AnoGAN Framework . . . 37
3.2 Energy Based Generative Adversarial Networks . . . 41

4 Architectural Improvements **45**
4.1 SEM Image Dataset 45
4.2 Analysis of Aforementioned Approaches 47
4.2.1 Stabilization of Adversarial Training 47
4.2.2 Convergence of Encoder Training 50
4.2.3 Encoded Energy Based Generative Adversarial Network 53
4.2.4 Anomaly Score Computation 56
4.3 Sequentially Encoded Energy Based Generative Adversarial Network 57

5 Experimental Results **61**
5.1 Experiment Settings 61
5.1.1 Performance Metrics 61
5.2 Pure GAN Model Analysis 62
5.3 Autoencoder Variant Model Analysis 62
5.4 Improved Model Analysis 62
5.5 Discussion of Experiment Results 62

6 Conclusion and Future Work **67**

A Model Implementation Details **69**
A.1 AnoGAN Implementation 69
A.2 BiGAN Implementation 70
A.3 ALAD Implementation 70
A.4 GANomaly Implementation 72
A.5 Skip-GANomaly Implementation 73
A.6 ENCEBGAN Implementation 73
A.7 SENCEBGAN Implementation 74

Bibliography **77**

List of Figures

21 GAN architecture overview 9
22 Simple Autoencoder architecture 15
23 Stacked Autoencoder with multiple layers 15
24 ALI architecture overview 20
25 BiGAN architecture overview 21
26 ALAD architecture overview 31
27 GANomaly architecture overview 33
28 Skip GANomaly architecture overview [3] 35

31 F-AnoGAN Framework Overview [49] 38
32 F-AnoGAN Training Strategies [49] 39
33 Anomaly Score computations for both training methods [49] . . 40
34 EBGAN Model Structure [58] 42

41 Part of Training Dataset from the SEM Image Dataset [51] . . . 46
42 Normal and Anomalous region patches for the training and testing 46
43 Training information for the Pure GAN models. For graphs, x axis is the number of epochs and the y axis is the loss value . . 49
44 Training graphs of pure GAN models that implement encoder network and the first iteration of the proposed network 51
45 Reconstructed samples from the pure GAN models. Upper row is the given query image and the bottom row is their reconstructions 52
46 ENCEBGAN Model Overview 54
47 Training graphs and qualitative examples from ENCEBGAN Model 55
48 Reconstruction examples of Autoencoder Variant Models 56
49 SENCEBGAN Model Overview 57

List of Tables

51 Ablation study for AnoGAN to test the effect of various training improvements for stabilization. 63
52 Ablation study for BiGAN to test the effect of various training improvements for stabilization. 63
53 Ablation study for ALAD to test the effect of various training improvements for stabilization. 64
54 Ablation study for GANomaly to test the effect of various training improvements for stabilization. 64
55 Ablation study for Skip-GANomaly to test the effect of various training improvements for stabilization. 65

A1 Architecture and Hyperparameters of AnoGAN Model 69
A2 Architecture and Hyperparameters of BiGAN Model 70
A3 Architecture and Hyperparameters of ALAD Model 71
A4 Architecture and Hyperparameters of GANomaly Model 72
A5 Architecture and Hyperparameters of Skip-GANomaly Model . 73
A6 Architecture and Hyperparameters of ENCEBGAN Model . . . 73
A7 Architecture and Hyperparameters of SENCEBGAN Model . . 74

CHAPTER 1

Introduction

Introduction will be written

Lorem ipsum dolor sit amet, consectetuer adipiscing elit. Ut purus elit, vestibulum ut, placerat ac, adipiscing vitae, felis. Curabitur dictum gravida mauris. Nam arcu libero, nonummy eget, consectetuer id, vulputate a, magna. Donec vehicula augue eu neque. Pellentesque habitant morbi tristique senectus et netus et malesuada fames ac turpis egestas. Mauris ut leo. Cras viverra metus rhoncus sem. Nulla et lectus vestibulum urna fringilla ultrices. Phasellus eu tellus sit amet tortor gravida placerat. Integer sapien est, iaculis in, pretium quis, viverra ac, nunc. Praesent eget sem vel leo ultrices bibendum. Aenean faucibus. Morbi dolor nulla, malesuada eu, pulvinar at, mollis ac, nulla. Curabitur auctor semper nulla. Donec varius orci eget risus. Duis nibh mi, congue eu, accumsan eleifend, sagittis quis, diam. Duis eget orci sit amet orci dignissim rutrum.

Nam dui ligula, fringilla a, euismod sodales, sollicitudin vel, wisi. Morbi auctor lorem non justo. Nam lacus libero, pretium at, lobortis vitae, ultricies et, tellus. Donec aliquet, tortor sed accumsan bibendum, erat ligula aliquet magna, vitae ornare odio metus a mi. Morbi ac orci et nisl hendrerit mollis. Suspendisse ut massa. Cras nec ante. Pellentesque a nulla. Cum sociis natoque penatibus et magnis dis parturient montes, nascetur ridiculus mus. Aliquam tincidunt urna. Nulla ullamcorper vestibulum turpis. Pellentesque cursus luctus mauris.

Nulla malesuada porttitor diam. Donec felis erat, congue non, volutpat at, tincidunt tristique, libero. Vivamus viverra fermentum felis. Donec nonummy pellentesque ante. Phasellus adipiscing semper elit. Proin fer-

mentum massa ac quam. Sed diam turpis, molestie vitae, placerat a, molestie nec, leo. Maecenas lacinia. Nam ipsum ligula, eleifend at, accumsan nec, suscipit a, ipsum. Morbi blandit ligula feugiat magna. Nunc eleifend consequat lorem. Sed lacinia nulla vitae enim. Pellentesque tincidunt purus vel magna. Integer non enim. Praesent euismod nunc eu purus. Donec bibendum quam in tellus. Nullam cursus pulvinar lectus. Donec et mi. Nam vulputate metus eu enim. Vestibulum pellentesque felis eu massa.

Quisque ullamcorper placerat ipsum. Cras nibh. Morbi vel justo vitae lacus tincidunt ultrices. Lorem ipsum dolor sit amet, consectetuer adipiscing elit. In hac habitasse platea dictumst. Integer tempus convallis augue. Etiam facilisis. Nunc elementum fermentum wisi. Aenean placerat. Ut imperdiet, enim sed gravida sollicitudin, felis odio placerat quam, ac pulvinar elit purus eget enim. Nunc vitae tortor. Proin tempus nibh sit amet nisl. Vivamus quis tortor vitae risus porta vehicula.

Fusce mauris. Vestibulum luctus nibh at lectus. Sed bibendum, nulla a faucibus semper, leo velit ultricies tellus, ac venenatis arcu wisi vel nisl. Vestibulum diam. Aliquam pellentesque, augue quis sagittis posuere, turpis lacus congue quam, in hendrerit risus eros eget felis. Maecenas eget erat in sapien mattis porttitor. Vestibulum porttitor. Nulla facilisi. Sed a turpis eu lacus commodo facilisis. Morbi fringilla, wisi in dignissim interdum, justo lectus sagittis dui, et vehicula libero dui cursus dui. Mauris tempor ligula sed lacus. Duis cursus enim ut augue. Cras ac magna. Cras nulla. Nulla egestas. Curabitur a leo. Quisque egestas wisi eget nunc. Nam feugiat lacus vel est. Curabitur consectetuer.

This document is organized as follows:

Chapter 2 outlines the state of the art methods that is used with this type of dataset. Chapter 3 explains other anomaly detection methods that benefit from the generative adversarial networks. Chapter 4 presents the anomaly detection problem throughly and reconstruction based approaches and the proposed approach for the problem. Experimental results are described in Chapter 5 and the conclusion and the future work is stated in chapter 6.

CHAPTER 2

State of the Art

This chapter is dedicated to the exploration of state of the art approaches in the fields relevant to the thesis. The organization of the chapter is the following: Section 2.1 will define what anomaly detection is and explain different approaches towards its solution. Section 2.2 will give necessary background information about Generative Adversarial Networks (GAN) and Autoencoder Networks. First the principles behind how GANs work will be presented then the autoencoder network architecture will be explained. This section is particularly significant to relate how different architectures that uses these networks function. In section 2.4, variety of architectures that is developed for anomaly detection will be studied as state of the art. How they are implemented and how they work in practise will be described.

2.1 Anomaly Detection

Anomaly detection can be defined as the task of classifying test data that differs in some respect from the data for the model that is availabla during training. [42] This definition correctly describes the task on the abstract level but does not clarify what anomaly actually is. Depending on the the application domain, anomalies can be referred to as outliers, novelties, discordant observations, exceptions, aberrations, surprises, peculiarities and contaminents.[14] Sometimes these can be used interchangebly in the context. These distinctions in the definition are primarily relies not only on the features of the data such as its dimentional complexity, its continuity and its format, but also on what is considered an anomaly for

that specific domain. This makes it harder to conceptualize the problem of anomaly detection with a general definition and a solution approach that can encompass all different domains.

In the rest of this section, I will explain different use cases for anomaly detection to show its impact on a broad spectrum of problems then the primary approach types to solve anomaly detection problem will be introduced.

The categorization threshold to define different application domains is constantly changing parallel to developments in the literature but the application areas of anomaly detection can be categorized down to these five general fields. [42] These are:

- IT Sector
- Healthcare informatics, medical diagnostics and monitoring
- Industrial Monitoring/ maintanence and damage detection
- Image processing/ Video Survailance
- Sensor Networks

IT Sector

Anomaly detection methods have a huge impact on the IT security systems, in which the objectives include network intrusion detection and fraud detection. [42] With the increased use of computerized systems and the inclusion of the internet based services to our daily lives, maintainability and the availability of these systems became much more important. For systems like these, anomaly is considered as a priority because it indicates significant but rare events and can prompt to critical actions to be taken in a wide range of application domain. [1]. For example a malicious process in a server may show increased use of resource from time to time that may be spotted as a type of anomaly in the system resource use patterns or the unusual amount of traffic on the network may indicate an intruder attack. [19] [27] Another aspect of the increased use of internet is its impact on the e-commerce field and dramatically growing online payment systems. This also includes a migration to internet banking in favor of the convenience of technology. As a result, insurance and credit card frauds, scams towards phone and mobile data usage, and phishing attacks targeting financial transactions become more and more severe. [20] In this context, behaviour of the consumer becomes the data. Transaction history, time spent between consecutive transactions and the geographic data can be used to construct a model to detect anomalies in the purchase patterns.

Healthcare

Healthcare and medical diagnostics is another domain for anomaly detection. Detecting anomalies in the progression of the disease symptoms is a crucial factor for treatment monitoring. [50] To aid diagnostics, interpretation of the patient data is also an important task for anomaly detection. Ability to differentiate between the instrumentation or recording errors and the actual clinically relevant change that may indicate a symptom should also be present in these anomaly detection systems. [42]. Patient data may include tabular information like the age, weight, blood test results, heart rate or respiratory rate [15][36] or medical image data [50].

Industrial Monitoring

Novelty detection became a huge part of the industrial automation systems from the quality control of the manufacturing progress to the performance maintanence of the equipments. Materials that have a complicated and delicate manufacturing process like cpu wafers [28] and nanofibrous materials [**Napoletano_2018**] may easily develop defects in the manufacturing pipeline.Therefore using anomaly detection is a viable option to reduce the wasted material and optimize the cost of producing the target product. Same principle also applies to the equipment used in these pipelines. Equipments and assets have the risk of deteorating over time due to the usage and wear [42]. For example heavy extraction machines that is used in the petroleum industry like turbomachines [37] needs constant supervision for damage prevention.

Image Processing

Image processsing methods has been used with anomaly detection methods extensively to detect novelty subjects or anomalies in the image or in a video stream. Detection in video data stream data is an important task for the surveilance systems that is used with the purpose of traffic control, security systems and search and rescue. [5]

Sensor Networks

With the improvements of the smart devices' involvement in our daily lives and the recent but promising developments in the field of internet of things, the definition of acquiring and processing data is evolved. Various types of sensors, especially wireless, are heavily used to collect huge amount of data to feed various systems such as surveillance, environmental monitoring, and disaster management. [54] These sensors usually used to create a network distributed over a large area with one or depending on the scale multiple sink nodes responsible for gathering information from the other sensors. In these distributed systems, sensors are used to compute or pre-

dict information depending on the problem. However the accuracy of these computations or predictions depends primarily on the quality of the sensor measurements and with this scale the instrumentation error is unavoidable. That's why anomaly detection tasks usually deployed on these systems to observe sensory faults and prevent malicious attacks. [42] [8]

Variety of approaches that belong to different sub domains of the machine learning, statistics , bayesian and information theory are used to solve anomaly detection problem for these aforementioned fields. All these different approaches in general tries to build a model or a representation of the training data which contains no anomalous samples (or very few) and assigns them an anomaly score or a label depending on the problem. At the inference stage, deviations from the constructed normality definition are detected using a predetermined anomaly threshold. These different approaches can be categorized into 5 main titles. These are:

- Probabilistic Anomaly Detection Methods
- Distance Based Anomaly Detection Methods
- Domain Based Anomaly Detection Methods
- Information Theoretic Anomaly Detection Methods
- Reconstruction Based Anomaly Detection Methods

Probabilistic approaches aim to estimate the generative probability density function of the data with the assumption that the input data is generated from an unknown probability distribution D, and learning this distribution gives us an idea about the representation of normality for the input data, training set. Anomaly (or novelty in some approaches) threshold then can be determined which has certain probabilistic interpretation and can be used to detect the anomaly on the inference stage. [42] Distance based methods are another type of modelling technique used to model the training data with a probability density function equivalent process. Including the K-Nearest neighbour based and clustering based methods, distance based methods rely on distance metrics between the data points to create a representation for normality. For example considering the K-NN aproach, data points in the training dataset are identified to have close neighbour points using the distance metrics while if a sample has a greater distance to the nearest normal point with a value above the determined anomaly threshold, that sample is identified as an anomaly. Domain based methods works by creating a boundry based on the structure of the training dataset. [42] These methods are usually insensitive to different sampling or the density properties because instead of learning the density of the data, the learn the boundary information to seperate the target class (anomalies) from the

normal data. Support Vector Machines (SVM) are the popular example for this approach. Information theoretic anomaly detection methods computes the total information content that resides in the training dataset. The main assumption is that anomalous samples present in the data significantly modifies the information content of the assumed normal dataset. Metrics for this approach are calculated using the entirety of the dataset and the subset that triggers the biggest discrapancy is identified as the anomaly.

Finally reconstruction based approaches which also is the focus of this thesis, model the underlying representation of the data and reconstructs it. Using the original input and the reconstructed output, these models define a reconstruction error tailored to the nature of the problem and the type of data and measures this error with respect to certain anomaly threshold. Since the modelled underlying data has the features specific to the training dataset, when the anomalous sample is feeded through this pipeline, its representation and consequently its reconstruction will be made poorly hence giving a greater reconstruction error.

2.1.1 Related Works

In this subsection, previous works and state of the art related to anomaly detection in images and proceed with particular case of SEM images will be listed. Proposed methods for anomaly detection for images can be grouped in reference-based and reference-free ones [14]. Reference-based methods compares the input image with a template image which is anomaly-free by definition and result of this comparison decides in run-time whether input includes anomalous component or not [60]. However, they are not feasible for considered SEM images where filament structures follow pseudo random rather than geometric pattern [12].

On the other hand, reference-free methods are more applicable because they can detect anomalies by using features that can consistently create varying responses for normal and anomaly regions [12]. This concept is also well-known as novelty detection [42].

This problem of particular dataset of SEM images previously studied in [12], [13] and [11] and these methods are based on learning a sparse dictionary that represents the normal regions and in run-time, if the input does not conform with the learned dictionary, it is detected as anomaly. Another approach that introduces convolutional neural networks is established by Napoletano et al. [39]. To extract feature for "normality" concept, they exploit pretrained network called ResNet which consists of residual networks

and trained by large number of images [25]. After feature extraction, for test phase, they create a dictionary by using K-means clustering to have the representation of normal regions.

Another powerful model for novelty detection problems is auto-encoders. Auto-encoders are quite useful tools to learn the dynamics of a distribution defined over images and to generate examples that corresponds to a sample on learned distribution. Therefore, they are easily deployed for the motivations of novelty detection as done in [4], [34] and [41]. Particularly, in Sabokrou et al.[46], leverages two staged network that is composed by auto-encoders and convolutional neural networks is explored for the novelty detection.

In the later sections, state of the art generative adversarial network based frameworks will be introduced. How the reconstruction loss is computed and anomaly score is formed will be explained in each framework.

2.2 Architectural Components

This section will explain the two main network types used in the state of the art anomaly detection frameworks in the following sections. Generative adversarial networks section will describe how the framework is formed, the intuition behind its adversarial training scheme. Autoencoder networks section will give an introductionary information to the subject and introduce different kinds of approaches that can be integrated into both the construction of the network and its training methodology.

2.2.1 Generative Adversarial Networks

One of the main objectives of the deep learning is to be able to create complex and high dimensional models that can capture the relations amongst the fundamental types of data that we perceive and be exposed to in our daily lives. This data can vary, it can be a visual information like an image, symbols in natural language or audio waveforms containing speech. Then we use these models to make machines make sense of the world we live in and exhibit what we call an intelligence. [9]

In the terms of statistical classification, also in machine learning (that consequentially includes deep learning) the main two approaches are called discriminative and generative modelling. Discriminative models maps the rich, complex sensory data to a class label, target so to speak to perform

the desired task. They try to learn the conditional probability distribution of the input data using the features of the data. The success behind this approach is the result of the improvements in the training, learning and generalization of these models. Backpropagation [55], dropout [53], and rectified linear units[21] are some of the examples of concepts that contribute to this success.

Generative models in that regard did not show a considerable promise as opposed to discriminative models mainly because of the type of problem they try to solve and computational difficulties regards to that solution. The generative models try to estimate the joint probability distribution of the high dimensional sensory input data to be able to generate data similar to input and its label with some variations which can be thought as imaginative. The main difficulty resides in the probabilistic computations that are hard to control in the maximum likelihood estimation. [23] [47]

Generative Adversarial Networks (GAN) are considered as one of the most significant breakthroughs in deep learning and generative modelling in the recent years. It is a framework that consists of two seperate modules. One of them is labelled as generator and the other is the discriminator. You can observe the example architecture in the figure 21.

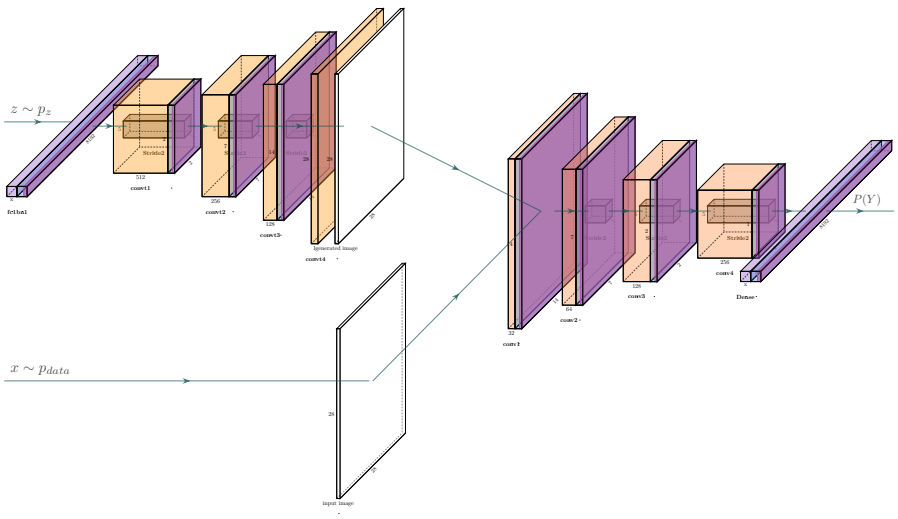

Figure 21 – GAN architecture overview

From this point on, "image" will be used to specify the type of the input and the target data because GAN frameworks are mainly designed to work with high dimensional spatial data like images so it will be consistent when

explaining the theorem and also the central focus of the thesis is on the spatial data.

The power of this framework comes from the adversarial nature of the training process. Simply put, the goal of the generator network is to create images similar to the input data by capturing the data distribution using a probabilistic model. On the other hand discriminator tries to detect fake (generated) images that is generated by generator from the real input images. We can represent this intuition with the following two player minimax game with the value function $V(G, D)$ in equation 2.3. [23]

$$p_{\text{data}}(x) : x \in \Omega_X \quad \text{(Distribution of the data)} \tag{2.1}$$

$$p_z(z) : z \in \Omega_Z \quad \text{(Distribution of the noise)} \tag{2.2}$$

$$V(G, D) = \mathbb{E}_{\boldsymbol{x} \sim p_{\text{ data}}(\boldsymbol{x})}[\log D(\boldsymbol{x})] + \mathbb{E}_{\boldsymbol{z} \sim p_{\boldsymbol{z}}(\boldsymbol{z})}[\log(1 - D(G(\boldsymbol{z})))] \tag{2.3}$$

The training objective criterion for the discriminator is to maximize the expected log-likelihood of classifying the input data as real. p_{data} represents the distribution of the input. Since the generated data should be classified as fake by the discriminator, the output of the second term is flipped. The Generator's purpose is to "fool the discriminator". Hence its objective criterion is to minimize the expected log likelihood of discriminator classifying generated image sample as fake. We can interpret this equation as two seperate objective functions with different training criterions :

$$\min_G V(G, D) = \mathbb{E}_{\boldsymbol{z} \sim p_{\boldsymbol{z}}(\boldsymbol{z})}[\log(1 - D(G(\boldsymbol{z})))] \tag{2.4}$$

$$\max_D V(G, D) = \mathbb{E}_{\boldsymbol{x} \sim p_{\text{ data}}(\boldsymbol{x})}[\log D(\boldsymbol{x})] + \mathbb{E}_{\boldsymbol{z} \sim p_{\boldsymbol{z}}(\boldsymbol{z})}[\log(1 - D(G(\boldsymbol{z})))] \tag{2.5}$$

While this equation describes the relation between the two adversaries, it does not provide a definite explanation how this training objective finds equilibrium and whether that equilibrium also provides us with the optimal generator or not. For this analysis we will use bottom up approach and prove the theorem mentioned in the original GAN approach [23].

Theorem 2.2.1. *The global minimum of the virtual training criterion $C(G)$ is achieved iff $p_g = p_{data}$. At that point, $C(G)$ achieves the value $-log(4)$.*

We start by defining the term expected value of a function.

Definition 2.2.1. $E(f(x))$ of some function $f(x)$ with respect to certain probability distribution $p(x)$ is called the expected value of a function and it is expressed like

$$E_{x\sim p_x} = \int p(x)f(x)dx \tag{2.6}$$

So the minimax game equation can be expressed like this:

$$V(G,D) = \int_x p_{\text{data}}(\boldsymbol{x})log(D(\boldsymbol{x}))dx + \int_z p_z(\boldsymbol{z})log(1-D(G(\boldsymbol{z})))dz \tag{2.7}$$

For generator to sample an image good enough to fool the discriminator, framework needs to learn the implicitly created sample distribution p_g by the generator G. Framework defines a prior noise distribution $z \sim p_z$, isotropic gaussian distribution with zero mean and unit variance to learn the distribution p_g (Different distributions are also considered). Next we use the LOTUS theorem.

Theorem 2.2.2. *Law of the unconscious statistician (LOTUS) theorem is used to compute the expected value of a function $g(x)$ of a random variable X when one knows the probability distribution of X but does not know the probability distribution of $g(x)$. [44]*

The expected value of a function $g(x)$ then can be expressed like:

$$\mathrm{E}[g(X)] = \sum_x g(x)f_X(x) \tag{2.8}$$

$f_X(x)$ being the proability distribution of the random variable X.

Using this law we can write the equation $V(G,D)$.

$$z \sim p_z, \quad G(z) = x, \quad x \sim p_g \tag{2.9}$$

$$V(G,D) = \int_x p_{\text{data}}(\boldsymbol{x})log(D(\boldsymbol{x})) + p_g(\boldsymbol{x})log(1-D(\boldsymbol{x}))dx \tag{2.10}$$

For the Discriminator D, the value of the training criterion should be maximized. That basically means the derivative of the function of this expected value expression should be equal to zero. We write the function by reversing the process of the equation 2.6.

$$f(p_{\text{data}}, p_g) = p_{\text{data}}(\boldsymbol{x})\log(D(\boldsymbol{x})) + p_g(\boldsymbol{x})\log(1-D(\boldsymbol{x})) \tag{2.11}$$

$$f' = p_{\text{data}}(\boldsymbol{x})\frac{1}{D(\boldsymbol{x})\ln(C)} - p_g(\boldsymbol{x})\frac{1}{(1-D(\boldsymbol{x}))\ln(C)} \tag{2.12}$$

$$f' = 0 \tag{2.13}$$

$$p_{\text{data}}(\boldsymbol{x})(1-D(\boldsymbol{x}))\ln(C) = p_g(\boldsymbol{x})D(\boldsymbol{x})\ln(C) \tag{2.14}$$

$$(p_{\text{data}}(\boldsymbol{x}) + p_g(\boldsymbol{x}))D(\boldsymbol{x}) = p_{\text{data}}(\boldsymbol{x}) \tag{2.15}$$

$$D^*_G(\boldsymbol{x}) = \frac{p_{\text{data}}(\boldsymbol{x})}{(p_{\text{data}}(\boldsymbol{x}) + p_g(\boldsymbol{x}))} \tag{2.16}$$

This is the optimal discriminator D with the fixed G. By deriving this value, we show that the maximum value the Discriminator can reach is the result of the equation 2.16. Next, we reformulate our $V(G,D)$ to analyze for the training criterion of the generator G.

$$C(G) = \max_D V(G,D) \tag{2.17}$$

$$= \mathbb{E}_{\boldsymbol{x}\sim p_{\text{data}}}[\log D^*_G(\boldsymbol{x})] + \mathbb{E}_{\boldsymbol{z}\sim p_{\boldsymbol{z}}}[\log(1 - D^*_G(G(\boldsymbol{z})))] \tag{2.18}$$

$$= \mathbb{E}_{\boldsymbol{x}\sim p_{\text{data}}}[\log D^*_G(\boldsymbol{x})] + \mathbb{E}_{\boldsymbol{x}\sim p_g}[\log(1 - D^*_G(\boldsymbol{x}))] \tag{2.19}$$

$$= \mathbb{E}_{\boldsymbol{x}\sim p_{\text{data}}}\left[\log\frac{p_{\text{data}}(\boldsymbol{x})}{P_{\text{data}}(\boldsymbol{x}) + p_g(\boldsymbol{x})}\right] + \mathbb{E}_{\boldsymbol{x}\sim p_g}\left[\log\frac{p_g(\boldsymbol{x})}{p_{\text{data}}(\boldsymbol{x}) + p_g(\boldsymbol{x})}\right] \tag{2.20}$$

In the theorem the equality $p_{\text{data}} = p_g$ is given. By applying this equality we get $D^*_G(\boldsymbol{x}) = \frac{1}{2}$. By putting this to our equation we get

$$C(G) = \log(\frac{1}{2}) + \log(\frac{1}{2}) = -\log(4)$$

. To verify that this value is indeed the global point for the equation we apply the following substraction:

$$C(G) - (-\log(4)) = \int p_{\text{data}}\left[\log\frac{p_{\text{data}}}{p_{\text{data}} + p_g} + \log 2\right] + \int p_g\left[\log\frac{p_g}{p_{\text{data}} + p_g} + \log 2\right]$$

$$C(G) - (-\log(4)) = \int p_{\text{data}} \left[\log \frac{2p_{\text{data}}}{p_{\text{data}} + p_g} \right] + \int p_g \left[\log \frac{2p_g}{p_{\text{data}} + p_g} \right]$$

$$C(G) - (-\log(4)) = \int p_{\text{data}} \left[\log \frac{p_{\text{data}}}{(p_{\text{data}} + p_g)/2} \right] + \int p_g \left[\log \frac{p_g}{(p_{\text{data}} + p_g)/2} \right] \tag{2.21}$$

To interpret this result we introduce 2 divergence definitions.

Definition 2.2.2. The Kullback-Leibler divergence is the measure of how one probability distribution is different from the other one. Its general definition is

.

$$D_{KL}(P\|Q) = \int p(x) \log \frac{p(x)}{q(x)} \tag{2.22}$$

More generally if P and Q are probability measures[1]over a dataset X, and measure P is absolutely continous with respect the Q, then the Kullback-Leibler divergence can also be defined as in equation 2.23

$$D_{\text{KL}}(P\|Q) = \int_{\mathcal{X}} \log \left(\frac{dP}{dQ} \right) dP \tag{2.23}$$

where $\frac{dP}{dQ}(f_{PQ})$ is the Radon-Nikodym derivative [10]. The defining property of radon-nikodym property that ties to the probability measure is that

$$P(R) = \int_R f_{PQ} dQ \tag{2.24}$$

The RN derivative $f_{PQ} : \Omega \mapsto \mathcal{R}_{\geq 0}$ is defined for any measures P and Q on a space Ω such that P is absolutely continous with respect to Q. In other words, for any $R \subseteq \Omega : P(R) > 0 \implies Q(R) > 0$. [10]

Definition 2.2.3. Jensen-Shannon divergence is a measure of similarity between different probability distributions. Its major difference from the KL divergence is that it is always symmetric and it always has a non-negative value. The General definition is provided in equation 2.25.

[1]a probability measure is a real-valued function defined on a set of events in a probability space that satisfies measure properties such as *countable additivity*[45]

$$JSD(P\|Q) = \frac{1}{2}D_{KL}(P\|M) + \frac{1}{2}D_{KL}(Q\|M) \tag{2.25}$$

Using this divergence measures we can rewrite our equation as this:

$$C(G) = -\log(4) + KL\left(p_{\text{ data}} \| \frac{p_{\text{ data}} + p_g}{2}\right) + KL\left(p_g \| \frac{p_{\text{ data}} + p_g}{2}\right) \tag{2.26}$$

$$C(G) = -\log(4) + 2 \cdot JSD\left(p_{\text{ data}} \| p_g\right) \tag{2.27}$$

Considering Jensen-Shannon divergence is always non-negative and zero only when the distributions are identical, we can conclude the proof by stating that the global minimum point of $C^*(G) = -\log(4)$ is only achieved when $p_{\text{data}} = p_g$.

Intuition behind the adversarial training of this framework is important because all the subsequent approaches that will be discussed in the thesis that use GAN's fundamentally benefit from this framework to train their networks. As we will see in the BiGAN (section 2.3.2) and similar models, addition of encoder network changes the overall minimax game played by the adversary networks but underlying logic still depends on the value function of the GANs.

2.2.2 Autoencoder Networks

Autoencoder network is a type of neural network that is trained to copy its input data to output. [22] In its simplest form, it can be defined as a feedforward, non- recurrent network similar to multilayer perceptrons like in figure 22.

Internally, it consists of a hidden layer that describes the representation (code) learned from the input data. The connections from the hidden layer to the output layer transforms the hidden representation into the output data with the same dimensionality as the input. Rather that trying to reconstruct the given data, autoencoders are mainly used to learn the representation about the data to extract meaningful features and to reduce the dimensionality of the data while keeping the relevant information as an alternative to principal component analysis.

With the increased complexity of the data present, this architecture can be extended to capture more complex feature representations by stacking similar but varying encoder and decoder layers on top of each other. Gen-

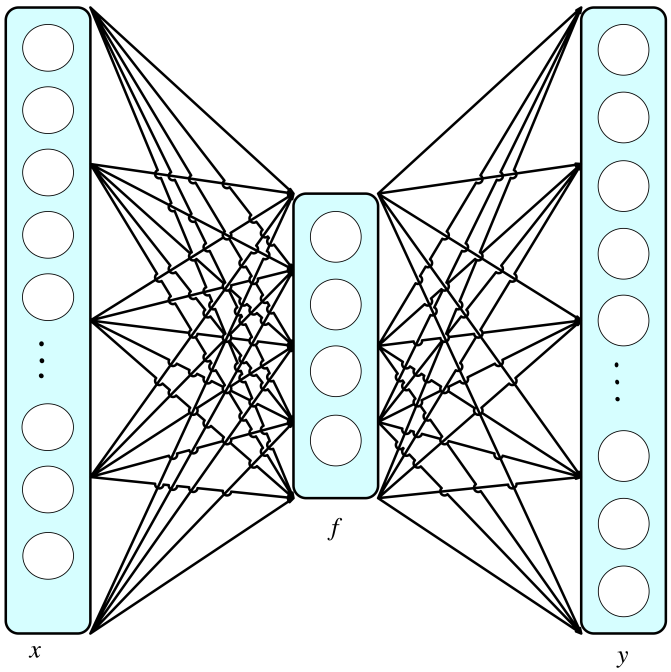

Figure 22 – Simple Autoencoder architecture

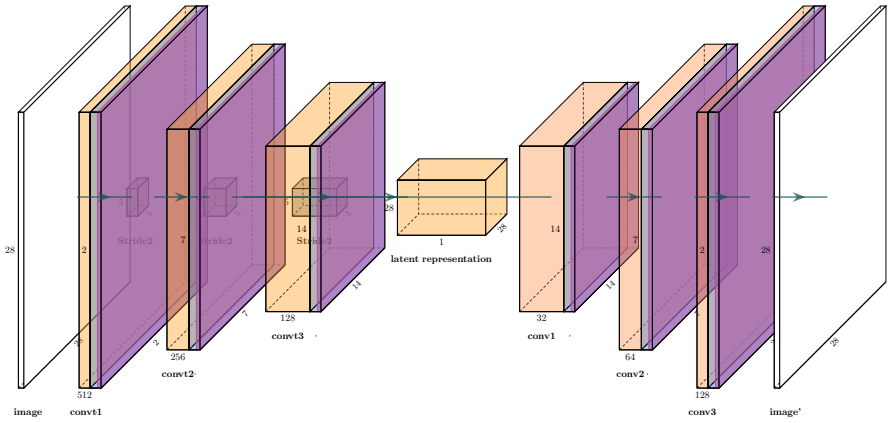

Figure 23 – Stacked Autoencoder with multiple layers

erally first layers learn the more basic features of the data and as the layers are stacked, more concentrated and complex features can be learnt in the code section of the autoencoder, the end of the encoder module. These

architectures are mainly referred to as deep autoencoders because of the increased level of hidden layers present in the model depicted in figure 23, just like in deep learning.

Learning rationale of the autoencoders can be visualized with a pair of weighted layer computation functions like in the multilayer perceptrons. Assume that we have two transition functions that defines the relationship between the real data and the intermediate representation as the result of the encoder network:

$$\phi : X \mapsto F$$
$$\psi : F \mapsto X$$

We can define the intermediate representation computation and the reconstruction of the input data with the following equations:

$$z = \sigma(Wx + b), \quad x \sim X \in \mathbb{R}^d, \quad z \sim F \in \mathbb{R}^p \tag{2.28}$$
$$x' = \sigma'(W'z + b') \tag{2.29}$$

The primal training objective for the autoencoders is the reconstruction loss. Depending on the architecture of the decoder or the desired task, the source of the parameters for the objective function can change. Autoencoder learns the representation of the data by minimizing the reconstruction loss.

$$\phi, \psi = \underset{\phi,\psi}{\operatorname{argmin}} \|X - (\psi \circ \phi)X\| \tag{2.30}$$
$$L(x, x') = \left\|x - x'\right\|^2 = \left\|x - \sigma'(W'\sigma(Wx + b) + b')\right\|^2 \tag{2.31}$$

With enough model capacity and training time, autoencoder might learn to copy the input perfectly. This reduces the functionality of the encoder-decoder modules to a identity function:

$$x \sim X \in \mathbb{R}^d, \quad \psi(\phi(x)) = x$$

This is generally an unwanted outcome. To overcome this problem, autoencoders are designed to learn the representation of the data imperfectly. [22] This is achieved by how the encoder module learns to compress the data to a meaningful representation. These 3 types of autoencoder models can give an idea about how the architecture can be changed to alter the amount of information that can be extracted from the data. These are:

- Undercomplete Autoencoders
- Regularized Autoencoders
- Denoising Autoencoders

The undercomplete autoencoders reduce the dimension size of the latent representation. Learning purposefully insufficient representation forces autoencoder to keep the most salient features about the data. The training objective function is the reconstruction loss which presented in equation 2.30. If the computation of this function is linear, then the autoencoder mimics the behaviour of a principal component analysis method. When the encoder transition ϕ and the decoder transition ψ is designed to have a nonlinear nature, then the autoencoder has the ability to capture more complex reprensetation of the data, more powerful approach than the PCA. But this has the risk of again, causing autoencoder to replicate the input data perfectly and becoming an identity function $x' = \psi(\phi(x))$. Regularized autoencoders' design difference is that their latent representation layer usually has same or higher dimensional power (more neurons from the perspective of multilayer perceptrons). To acquire a similar performance like undercomplete variants, they regularize the loss function with the potential properties of the data distribution such as robustness to the noise or the sparsity of the representation. Prioritizing which aspects of the data will be used as a regularizer term for the objective function is a task dependent problem. [22]. Denoising autoencoders tries to solve a different problem to achieve a good representation.

$$\hat{x} = x + \epsilon : x \sim X \in \mathbb{R}^d, \quad \epsilon \sim \mathcal{N}(\mu, \sigma^2)$$

The input data is corrupted with some kind of noise, gaussian etc. Denoising autoencoders tries to reconstruct the data and undo this corruption by minimizing this updated loss with the difference of the $\hat{x}$

$$L(x, \psi(\phi(\hat{x})))$$

2.3 GAN Based Anomaly Detection Methods

Anomaly detection on spatial data using reconstruction based methods primarily converges around variational autoencoders and other stuff. The GAN based approaches in this field are relatively new. In the following subsections, I will explain the approaches that can be considered as the state of the art for this problem in the order of their complexity and incremental improvements. Each approach will be evaluated by their problem

description, the type of data they use, model architecture and anomaly score computation.

2.3.1 AnoGAN

AnoGAN model is the first approach that utilizes GANs for the anomaly detection task. [50] It focuses on the problem of detecting anomalous regions in optical coherence tomography images. Images containing retinal fluid or hyperreflective foci (indicator of disease progression in various retinal diseases) are identified as anomalous examples. The main motivation to use GANs to obtain a model which represents normal anatomical variability of the data is that previous supervised approaches involves training a model with a large dataset using annotated examples of known markers. Relying on vocabulary of markers may limit the predictive power of the model as the image contains much more relevant information than the marker and extensive supervised training is a problem because it means that every stage of the disease requires an extensive training with annotated examples such as labeled lesions which may decrease limit of exploiting imaging data for treatment decisions. [50].

The framework consists of 2 parts. First part is the GAN module, generator and discriminator networks. Their architecture is inspired by the original DCGAN architecture[43]. The objective function of the GAN is the same of the equation 2.3. During the training the generator enhances its ability to generate more realistic retinal images while the discriminator learns the diagnose the real and the generated sample more efficiently.

The second part of the framework is about the inverse mapping of the noise to the image. We know from the GANs training procedure that when the adversarial training is completed, the generator network has learnt the distribution p_g that is theoretically very similar to the input data distribution p_{data}. (I state "theoretically" explicitly because depending on the configuration of the GAN and the data that is used, this may differ significantly in practise. This aspect of the learning will be mentioned in the latter approaches.) Even though with the trained generator,

$$G(z) = z \mapsto x, x \sim p_{\text{data}}$$

the GAN framework does not learn the inverse mapping from the image to the noise. AnoGAN framework aims to find the noise sample $z\prime$ from the query image (normal or anomalous) such that the generated image $G(z\prime)$ is visually the most similar one to the query image. This is essential for

the anomaly detection task. $z\prime$ is sampled randomly as initialization. Then the $G(z\prime)$ is computed and based on the defined loss function gradients the coefficients of $z\prime$ is updated using backpropagation. This procedure is repeated for a number of epochs to obtain the final value of the $z\prime$.

The loss function for the inverse mapping is defined as the combination of two seperate losses. Residual loss is responsible for enforcing visual similarity between the generated image $G(z\prime)$ and the query image x.

$$L_R(z_\gamma) = \sum \|x - G(z_\gamma)\| \tag{2.32}$$

Discrimination loss on the other hand enforces the generated image $G(z\prime)$ to lie on the manifold X of image x.

$$L_D(z_\gamma) = \sum \|f(x) - f(G(z_\gamma)\| \tag{2.33}$$

There are two different implementation for the discriminaton loss. One with sigmoid cross entropy which is from the original GAN implementation [23] and one with feature matching [48] which uses the last layer of the discriminator rather than the output to compute the loss. Using this loss allows them to use discriminator not as a classifier but as a feature extractor. Using both residual and discriminaton loss, the total loss function is defined as :

$$L(z_\gamma) = (1-\lambda) \times L_R(\boldsymbol{z_\theta}) + \lambda \times L_D(\boldsymbol{z_\gamma})$$

Only the coefficients of z is adapted via backpropagation. The trained weights of the generator and discriminator are fixed in this stage. [50]

The Anomaly detection task uses same loss functions to compute the anomaly score.

$$A(x) = (1-\lambda) \times R(\boldsymbol{x}) + \lambda \times D(\boldsymbol{x})$$

The $R(x)$ is the residual score value and the $D(x)$ is the discriminaton score value at the last update iteration of the inverse mapping procedure, respectively. The model outputs a larger anomaly score $A(x)$ for anomalous samples though smaller score means that very similar image is seen during the training of the GAN.

This model is the first model that integrates generative adversarial networks to an anomaly detection framework. The mapping from latent representation to image data is completely dependent on the architecture of the GAN and its training parameters. The disadvantageous aspect of this approach is the inference. For each query image framework approximates

the latent representation vector using backpropagation steps which makes the whole process significantly slow compared to the other approaches. Improvements to this framework is discussed in the Latest Developements chapter (3.1). The experiment results and the implementation details will be covered in chapter 5.

2.3.2 BiGAN and ALI

BiGAN (Bidirectional Generative adversarial Networks) [17] and ALI (Adversarially Learned Inference) [18] are two models that independent from each other but focuses on the same problem. They investigate to acquire efficient inference method from data to latent space by using encoders in the adversarial training framework of GANs. They emphasize learning the inverse mapping for the auxilary supervised tasks such as classification, segmentation and discrimination. The only difference between the models is that the BiGAN uses a deterministic network for the encoder while ALI uses a stochastic network. I will first briefly explain the original architecture of the ALI and continue to present the framework in detail using BiGAN instead since their explanation for the model is more consistent with the GAN framework. Furthermore I will discuss how this architecture can be used for anomaly detection. In the original papers, anomaly detection has not been explored as an auxilary supervised task but the later models like in section 2.3.3 or in section 2.3.4, used these architectures as a state of the art comparison in terms of both foundation and performance measure hence their use of anomaly detection will also be discussed.

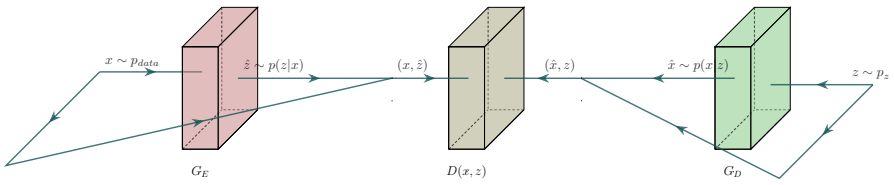

Figure 24 – ALI architecture overview

Aligan architecture is depicted as a generator and a discriminator in figure 24. The significant change in ALI is that the generator is the combination of decoder network and an encoder network. Encoder represents the joint distribution $p_E(x, z)$ which has the marginal $p_{\text{data}(x)}$ and decoder represents the joint distribution $p_D(x, z)$ with the marginal $p_z(z)$ which represents the factorized noise distribution (generally $\mathcal{N}(0, 1)$). The objective function of the ALI is to match these two joint distributions. Successing

in this goal also ensures the match of the marginals and the conditional distributions $p(z|x)$ and $p(x|z)$. Discriminator is also modified to support this new objective function. It is trained to distinguish between the joint pairs $(x, \hat{z} = G_E(x))$ and $(\hat{x} = G_D(z), z)$ as data and noise.

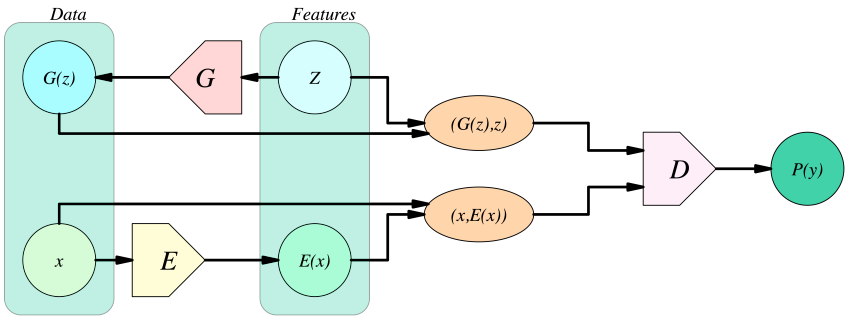

Figure 25 – BiGAN architecture overview

BiGAN architecture model is presented in figure 25. The architectures are theoretically identical with the exception of the encoder network choice in practise. BiGAN experiments are conducted with a deterministic network whilst ALI framework used a stochastic network. Apart from the generator, BiGAN also trains the encoder network in an adversarial manner. Same objective function used in GAN provides the relationship between the generator and encoder that $G = E^{-1}$ and vice versa. This invertibility is the key aspect of the model and the other frameworks to provide an efficient inference with reliable sampling. We Know from the section 2.2.1 that:

$$G : \Omega_z \mapsto \Omega_x$$

We define the Encoder with the reverse of that transition:

$$E : \Omega_x \mapsto \Omega_z$$

Since this framework accepts the networks as deterministic we also redefine the distributions for generator and encoder networks:

$$p_G(x|z) = \delta(x - G(z))$$
$$p_E(z|x) = \delta(z - E(x))$$

The objective function of the framework can be characterized as:

$$\min_{G,E} \max_{D} V(D,E,G) \tag{2.34}$$

where

$$V(D,E,G) := \mathbb{E}_{\mathbf{x}\sim p_{\mathbf{X}}} \underbrace{\left[\mathbb{E}_{\mathbf{z}\sim p_E(\cdot|\mathbf{x})}[\log D(\mathbf{x},\mathbf{z})]\right]}_{\log D(\mathbf{x},E(\mathbf{x}))} + \mathbb{E}_{\mathbf{z}\sim p_{\mathbf{Z}}} \underbrace{\left[\mathbb{E}_{\mathbf{x}\sim p_G(\cdot|\mathbf{z})}[\log(1-D(\mathbf{x},\mathbf{z}))]\right]}_{\log(1-D(G(\mathbf{z}),\mathbf{z}))} \tag{2.35}$$

To prove that the encoder is the inverse of the generator, optimal discriminator needs to be determined.[17] The joint distributions of the generator and encoder can be illustrated s the marginals of the data and the noise and related conditional probability distributions:

$$p_{GZ}(x,z) := p_G(x|z)p_Z(z) \tag{2.36}$$

$$p_{EX}(x,z) := p_E(z|x)p_X(x) \tag{2.37}$$

The joint latent space and the data for the problem can also be illustrated as a joint representation.

$$\Omega := \Omega_X \times \Omega_Z$$

For the region $R \subseteq \Omega$ probability measures[30] of encoder and generator is defined in equation 2.38 and 2.41 respectively.[17]

$$\begin{aligned} P_{E\mathbf{X}}(R) := & \int_{\Omega} p_{E\mathbf{X}}(\mathbf{x},\mathbf{z})\mathbf{1}^2_{[(\mathbf{x},\mathbf{z})\in R]}\mathbf{d}(\mathbf{x},\mathbf{z}) = \\ & \int_{\Omega_{\mathbf{X}}} p_{\mathbf{X}}(\mathbf{x}) \int_{\Omega_{\mathbf{Z}}} p_E(\mathbf{z}|\mathbf{x})\mathbf{1}_{[(\mathbf{x},\mathbf{z})\in R]}\mathbf{dzdx} \end{aligned} \tag{2.38}$$

$$= \int_{\Omega_{\mathbf{X}}} p_{\mathbf{X}}(\mathbf{x}) \left(\int_{\Omega_{\mathbf{Z}}} \delta(\mathbf{z} - E(\mathbf{x}))\mathbf{1}_{[(\mathbf{x},\mathbf{z})\in R]}\mathbf{dz} \right) \mathbf{dx} \tag{2.39}$$

$$= \int_{\Omega_{\mathbf{X}}} p_{\mathbf{X}}(\mathbf{x})\mathbf{1}_{[(\mathbf{x},E(\mathbf{x}))\in R]}\mathbf{dx} \tag{2.40}$$

$$
\begin{aligned}
P_{G\mathbf{Z}}(R) := \int_{\Omega} p_{G\mathbf{Z}}(\mathbf{x},\mathbf{z})\mathbf{1}_{[(\mathbf{x},\mathbf{z})\in R]}\mathrm{d}(\mathbf{x},\mathbf{z}) = \\
\int_{\Omega_{\mathbf{Z}}} p_{\mathbf{Z}}(\mathbf{z}) \int_{\Omega_{\mathbf{X}}} p_G(\mathbf{x}|\mathbf{z})\mathbf{1}_{[(\mathbf{x},\mathbf{z})\in R]}\mathbf{dxdz} \qquad (2.41)\\
= \int_{\Omega_{\mathbf{Z}}} p_{\mathbf{Z}}(\mathbf{z}) \left(\int_{\Omega_{\mathbf{X}}} \delta(\mathbf{x} - G(\mathbf{z}))\mathbf{1}_{[(\mathbf{x},\mathbf{z})\in R]}\mathbf{dx} \right) \mathbf{dz} \qquad (2.42)\\
= \int_{\Omega_{\mathbf{Z}}} p_{\mathbf{Z}}(\mathbf{z})\mathbf{1}_{[(G(\mathbf{z}),\mathbf{z})\in R]}\mathbf{dz} \qquad (2.43)
\end{aligned}
$$

Probability measures over regions on the image data $R_X \subseteq \Omega_X$ and the latent noise $R_Z \subseteq \Omega_Z$ can be similarly defined.

$$P_{\mathbf{X}}(R_{\mathbf{X}}) := \int_{\Omega_{\mathbf{X}}} p_{\mathbf{X}}(\mathbf{x})\mathbf{1}_{[\mathbf{x}\in R_{\mathbf{X}}]}\mathbf{dx} \qquad (2.44)$$

$$P_{\mathbf{X}}(R_{\mathbf{X}}) := \int_{\Omega_{\mathbf{X}}} p_{\mathbf{X}}(\mathbf{x})\mathbf{1}_{[\mathbf{x}\in R_{\mathbf{X}}]}\mathbf{dx} \qquad (2.45)$$

The optimal discriminator follows the same derivation from the GAN framework [23]. The Objective equation 2.35 can be reduced to the Jensen-Shannon divergence between joint distributions $P_{E\mathbf{X}}$ and $P_{G\mathbf{Z}}$ with the proof of the following propositions from the BiGAN [17].

Proposition 2.3.1. *For any E and G, the optimal discriminator $D^*_{EG} := \underset{D}{argmax} V(D,E,G)$ is the Radon-Nikodym derivative $f_{EG} := \frac{dP_{E\mathbf{X}}}{dP_{E\mathbf{X}}+dP_{G\mathbf{Z}}} : \Omega \mapsto [0,1]$ of measure $P_{E\mathbf{X}}$ with respect to measure $dP_{E\mathbf{X}} + dP_{G\mathbf{Z}}$.*

Proposition 2.3.2. *The encoder and generator's objective for an optimal discriminator $C(E,G) := \underset{D}{max} V(D,E,G) = V(D^*_{EG},E,G)$ can be rewritten in terms of the Jensen-Shannon divergence between the measures P_{EX} and P_{GZ} as $C(E,G) = 2D_{JS}(P_{E\mathbf{X}} \parallel P_{G\mathbf{Z}}) - \log 4$*

Discriminator is trained with both the encoder and generator network output. Therefore it is rational to assume that if we were to define a probability measure for discriminator . So we let P_{EG} be the average of the $P_{E\mathbf{X}}$ and $P_{G\mathbf{Z}}$.

$$P_{EG} = \frac{P_{E\mathbf{X}} + P_{G\mathbf{Z}}}{2} \qquad (2.46)$$

[2] Indicator function is a type of characteristic function that is used to indicate a membership on a subset X. It is denoted with bold **1** symbol.

Since both $P_{E\mathbf{X}}$ and $P_{G\mathbf{Z}}$ are continous with respect to the P_{EG}, the relationship of RN derivaties of f_{EG} and f_{GE} is defined accordingly:

$$f_{EG} := \frac{dP_{E\mathbf{X}}}{dP_{E\mathbf{X}} + dP_{G\mathbf{Z}}} \tag{2.47}$$

$$f_{GE} := \frac{dP_{G\mathbf{Z}}}{dP_{E\mathbf{X}} + dP_{G\mathbf{Z}}} \tag{2.48}$$

$$f_{EG} + f_{GE} := \frac{dP_{G\mathbf{Z}}}{dP_{E\mathbf{X}} + dP_{G\mathbf{Z}}} + \frac{dP_{E\mathbf{X}}}{dP_{E\mathbf{X}} + dP_{G\mathbf{Z}}} = \frac{d(P_{G\mathbf{Z}} + P_{E\mathbf{X}})}{d(P_{G\mathbf{Z}} + P_{E\mathbf{X}})} = 1 \tag{2.49}$$

Using the property of RN derivative (equation 2.24) we can transform the expected value function and rewrite the objective function of the BiGAN with a single probability measure.[17] [23]

$$\mathbb{E}_{\mathbf{x}\sim P}[g(\mathbf{x})] = \int_\Omega g\mathrm{d}P = \int_\Omega g\frac{\mathrm{d}P}{\mathrm{d}Q}\mathrm{d}Q = \int_\Omega g f_{PQ}\mathrm{d}Q = \mathbb{E}_{\mathbf{x}\sim Q}\left[f_{PQ}(\mathbf{x})g(\mathbf{x})\right] \tag{2.50}$$

We start by rewriting the original objective function with the joint probability distributions.

$$V(D,E,G) = \mathbb{E}_{(\mathbf{x},\mathbf{z})\sim P_{E\mathbf{X}}}[\log D(\mathbf{x},\mathbf{z})] + \mathbb{E}_{(\mathbf{x},\mathbf{z})\sim P_{G\mathbf{Z}}}[\log(1 - D(\mathbf{x},\mathbf{z}))] \tag{2.51}$$

Then the transformation described in equation 2.50 is applied.

$$= \mathbb{E}_{(\mathbf{x},\mathbf{z})\sim P_{EG}}[\underbrace{2f_{EG}}_{\frac{\mathrm{d}P_{EX}}{\mathrm{d}P_{EG}}}(\mathbf{x},\mathbf{z})\log D(\mathbf{x},\mathbf{z})] + \mathbb{E}_{(\mathbf{x},\mathbf{z})\sim P_{EG}}[\underbrace{2f_{GE}}_{\frac{\mathrm{d}P_{GZ}}{\mathrm{d}P_{EG}}}(\mathbf{x},\mathbf{z})\log(1 - D(\mathbf{x},\mathbf{z}))] \tag{2.52}$$

The final stage of the equation falls into a type of function $f(a,y) = a\log y + (1-a)\log(1-y)$ [17] which provides $\underset{y}{argmax} f(a,y) = a$ for any $a \in [0,1]$. Thus the optimal Discriminator $D^*_{EG} = f_{EG}$. That proves the first proposition.

$$= 2\mathbb{E}_{(\mathbf{x},\mathbf{z})\sim P_{EG}}\left[f_{EG}(\mathbf{x},\mathbf{z})\log D(\mathbf{x},\mathbf{z}) + f_{GE}(\mathbf{x},\mathbf{z})\log(1 - D(\mathbf{x},\mathbf{z}))\right] \tag{2.53}$$

$$= 2\mathbb{E}_{(\mathbf{x},\mathbf{z})\sim P_{EG}}\left[f_{EG}(\mathbf{x},\mathbf{z})\log D(\mathbf{x},\mathbf{z}) + (1 - f_{EG}(\mathbf{x},\mathbf{z}))\log(1 - D(\mathbf{x},\mathbf{z}))\right] \tag{2.54}$$

Second proposition can be proved with the same approach from GAN[23]

using the connection acquired from the first proposition. [17]

First the objective equation is rewritten with the optimal discriminator and its equivalent RN derivative. [17]

$$C(E,G) = \max_D V(D,E,G) = V\left(D^*_{EG},E,G\right) \tag{2.55}$$

$$= \mathbb{E}_{(\mathbf{x},\mathbf{z})\sim P_{E\mathbf{X}}}\left[\log D^*_{EG}(\mathbf{x},\mathbf{z})\right] + \mathbb{E}_{(\mathbf{x},\mathbf{z})\sim P_{G\mathbf{Z}}}\left[\log\left(1 - D^*_{EG}(\mathbf{x},\mathbf{z})\right)\right] \tag{2.56}$$

$$= \mathbb{E}_{(\mathbf{x},\mathbf{z})\sim P_{E\mathbf{X}}}\left[\log f_{EG}(\mathbf{x},\mathbf{z})\right] + \mathbb{E}_{(\mathbf{x},\mathbf{z})\sim P_{G\mathbf{Z}}}\left[\log f_{GE}(\mathbf{x},\mathbf{z})\right] \tag{2.57}$$

Then addition - subtraction of $\log 4$ is applied following the equation 2.21 to interpret the result as Jensen-Shannon divergence, hence proving the second proposition.

$$= \mathbb{E}_{(\mathbf{x},\mathbf{z})\sim P_{E\mathbf{X}}}\left[\log\left(2 f_{EG}(\mathbf{x},\mathbf{z})\right)\right] + \mathbb{E}_{(\mathbf{x},\mathbf{z})\sim P_{G\mathbf{Z}}}\left[\log\left(2 f_{GE}(\mathbf{x},\mathbf{z})\right)\right] - \log 4 \tag{2.58}$$

$$= \mathrm{D}_{\mathrm{KL}}\left(P_{E\mathbf{X}} \| P_{EG}\right) + \mathrm{D}_{\mathrm{KL}}\left(P_{G\mathbf{Z}} \| P_{EG}\right) - \log 4 \tag{2.59}$$

$$= \mathrm{D}_{\mathrm{KL}}\left(P_{E\mathbf{X}} \| \frac{P_{E\mathbf{X}} + P_{G\mathbf{Z}}}{2}\right) + \mathrm{D}_{\mathrm{KL}}\left(P_{G\mathbf{Z}} \| \frac{P_{E\mathbf{X}} + P_{G\mathbf{Z}}}{2}\right) - \log 4 \tag{2.60}$$

$$= 2\mathrm{D}_{\mathrm{JS}}\left(P_{E\mathbf{X}} \| P_{G\mathbf{Z}}\right) - \log 4. \square \tag{2.61}$$

The proposition 2.3.2 allows us to characterize the objective function of the BiGAN in terms of the Jensen-Shannon divergence but implicitly it also proves just like in equation 2.26 that the global minimum of the training criterion is only achieved with the equality of the probability measures $P_{E\mathbf{X}}$ and $P_{G\mathbf{Z}}$. Consequentailly this gives the optimality condition for both encoder and generator.

Theorem 2.3.1. *if E and G are an optimal encoder and generator, then $E = G^{-1}$ almost everywhere; that is, $G(E(x)) = x$ for P_X almost every $x \in \Omega_x$, and $E(G(z)) = z$ for P_z, almost every $z \in \Omega_z$. [17]*

The inversion property of the BiGAN framework is dependent on the factor of $P_{E\mathbf{X}}$ being equal to $P_{G\mathbf{Z}}$ in the optimal state. Let R^0_X be the region that the reconstructed image from the encoded noise is not equal to the input image and let R^0 be the region for the data, noise pairs which the data is also a member of the R^0_X. Using the optimal encoder and decoder, it can be proven that the probability measure for the region R^0_X is zero,

meaning that for almost every x in the region Ω_x, $G(E(x)) = x$ and vice versa.

$$R_X^0 := \{x \in \Omega_x : x \neq G(E(x))\} \tag{2.62}$$

$$R^0 := \{(x, z) \in \Omega : \mathbf{z} = E(x) \wedge x \in R_X^0\} \tag{2.63}$$

$$P_{\mathbf{X}}\left(R_{\mathbf{X}}^0\right) = \int_{\Omega_{\mathbf{X}}} p_{\mathbf{X}}(\mathbf{x}) \mathbf{1}_{[\mathbf{x} \in R_{\mathbf{x}}^0]} \mathbf{dx} \tag{2.64}$$

$$= \int_{\Omega_{\mathbf{X}}} p_{\mathbf{X}}(\mathbf{x}) \mathbf{1}_{[(\mathbf{x}, E(\mathbf{x})) \in R^0]} \mathbf{dx} \tag{2.65}$$

$$= P_{E\mathbf{X}}\left(R^0\right) \tag{2.66}$$

$$= P_{G\mathbf{Z}}\left(R^0\right) \tag{2.67}$$

$$= \int_{\Omega_{\mathbf{Z}}} p_{\mathbf{Z}}(\mathbf{z}) \mathbf{1}_{[(G(\mathbf{z}), \mathbf{z}) \in R^0]} \mathbf{dz} \tag{2.68}$$

$$= \int_{\Omega_{\mathbf{Z}}} p_{\mathbf{Z}}(\mathbf{z}) \mathbf{1}\left[\mathbf{z} = E(G(\mathbf{z})) \wedge G(\mathbf{z}) \in R_{\mathbf{X}}^0\right] \mathbf{dz} \tag{2.69}$$

$$= \int_{\Omega_{\mathbf{Z}}} \underbrace{p_{\mathbf{Z}}(\mathbf{z}) \quad \mathbf{1}_{[\mathbf{z}=E(G(\mathbf{z})) \wedge G(\mathbf{z}) \neq G(E(G(\mathbf{z})))]}}_{=0 \text{ for any } \mathbf{z}, \text{ as } \mathbf{z}=E(G(\mathbf{z})) \Longrightarrow G(\mathbf{z})=G(E(G(\mathbf{z})))} \quad \mathbf{dz} \tag{2.70}$$

$$= 0. \square \tag{2.71}$$

$$\tag{2.72}$$

Training of BiGAN framework is implemented using the same adversarial process of GANs. Encoder and generator network are trained together since they both try to minimize the objective. Each iteration is divied into two parts. First the discriminator is trained using the outputs from the encoder and generator with fixed weights, pushing the gradient of the function towards a positive step. Also the parameters of discriminator θ_D is updated. Then θ_E and θ_G the parameters of encoder and generator are updated concurrently with a negative direction in the gradient of the objective function. [17]

Loss functions for the training optimization and Anomaly score computation differs in terms of the type of approach, different from AnoGAN[50]. AnoGAN framework used the combination of the reconstruction loss (equation 2.32) and the discrimination loss (equation 2.33) both to infer z from

the query image and to compute the anomaly score. BiGAN framework's encoder is trained with the kind of function that is used to train the generator, sigmoid cross entropy. The advantage of the BiGAN is the reduced inference time to compute the anomaly score because the inferred noise from the query image $\hat{x}$ is the output from the generator $\hat{z} = E(\hat{x})$.

Anomaly score computation of BiGAN however, is the same approach used in AnoGAN. It uses a combination of the discriminaton loss and a reconstruction loss. The degree of norms used in the computation differs in the experiment stage to observe the behavior of the anomaly score. The Anomalous samples of the test dataset is determined by accepting the anomaly score that is greater then a predetermined threshold. This varies depending on the type of dataset and the dimensional complexity of the dataset the framework trained on.

2.3.3 ALAD

Adversarially Learned Anomaly Detection, or ALAD [57] is a framework designed for the anomaly detection task. It builds upon the idea of AnoGAN, using the base architecture from the AliGAN and BiGAN with additional improvements incorporated to increase the stabilization of the adversarial training in both discriminator module and encoder, generator pair. I will first describe the improvements introduced to the adversarial training framework and discuss their potential advantages over the previous approach. Then I will explain the ALAD architecture in detail. Lastly, learning of the model and the anomaly score computation choices will be discussed.

2.3.3.1 Spectral Normalization

Even tough the training of GAN works in practise, it may easily become unstable in certain conditions. For example, in high dimensional space, density ratio estimation of the discriminator network is often inaccurate and this results in generator networks fail to learn the dimensional structre of the target data distribution. [6] Consequently, when the support of the model distribution and the target distribution is disjoint, then the discriminator may become decently efficient classifying real data from the generated data sample. In this scenerio, the generator fails to learn to improve sample fake image data. Spectral Normalization is one of the recent proposed improvement methods to stabilize the weights of the discriminator network by bounding its gradients using Lipschitz continuity. [38]

Consider the optimal discriminator of $D(\boldsymbol{x},\theta) = \mathcal{A}(f(\boldsymbol{x},\theta))$ in equation 2.16. It takes the form :

$$D_G^*(\boldsymbol{x}) = \frac{q_{\text{ data}}(\boldsymbol{x})}{q_{\text{ data}}(\boldsymbol{x}) + p_G(\boldsymbol{x})} = \text{sigmoid}\left(f^*(\boldsymbol{x})\right), \quad \text{where } f^*(\boldsymbol{x}) = \log q_{\text{ data}}(\boldsymbol{x}) - \log p_G(\boldsymbol{x}) \tag{2.73}$$

Where $\mathcal{A}$ is an activation function corresponding to the divergence of distance measure of the user's choice (usually a sigmoid). With the derivative of:

$$\nabla_{\boldsymbol{x}} f^*(x) = \frac{1}{q_{\text{data}}(\boldsymbol{x})}\nabla_{\boldsymbol{x}} q_{\text{data}}(\boldsymbol{x}) - \frac{1}{p_G(\boldsymbol{x})}\nabla_{\boldsymbol{x}} p_G(\boldsymbol{x}) \tag{2.74}$$

This gradient function can be unbounded or even incomputable depending on the distribution. Spectral normalization is applied to introduce regularity condition to derivative $f(\boldsymbol{x})$. [38]

Discriminator function can be modified to apply this regularization to the objective function:

$$\begin{array}{l} \arg\max V(G,D) \\ \|f\|_{\text{Lip}} \leq K \end{array} \tag{2.75}$$

Where $\|f\|_{\text{Lip}}$ is depicted as the smallest value M such that:

$$\left\|f(\boldsymbol{x}) - f\left(\boldsymbol{x}'\right)\right\| / \left\|\boldsymbol{x} - \boldsymbol{x}'\right\| \leq M \tag{2.76}$$

for any x, x' with the norm being the l_2 norm. x_2 in X,[52]

Using the computation of the K-Lipschitz function of the each layer in discriminator, the spectral norm of each layer weight matrix can be normalized so the updated weights of the discriminator after each epoch of training becomes:

$$\overline{W}_{\text{SN}}(W) := W/\sigma(W) \tag{2.77}$$

2.3.3.2 Conditional Entropy (ALICE Framework)

The BiGAN framework in section 2.3.2 aims to learn both the mapping from the input image data to a latent representation with its encoder

module and the inverse of that mapping relation with its generator module. It acquires these mappings by training its enoder and generator modules together in an adversarial manner to learn a joint distribtuion depicted in equation 2.37 and 2.36. The problem suggested by the ALICE framework[35] is that learning the joint distribution alone doesn't help the model to reconstruct images necesarily faithful to the reproductions of the input data. [35] This is because the objective function is built only to match joint distributions of image and noise pairs at the same time potential dependency structures or correlations between two random variables within each joint repsentation is not specified or constrained. [35]

In order to reduce the identifiability issues associated with the objective of BiGAN, the conditionals $P_G(x|z)$ and $P_E(z|x)$ needs to be constrained and be under supervision using a paired samples from the domain Ω_x and Ω_z. Information-theoretic measure conditional entropy is used to provide this regularization.

Conditional entropy quantifies the amount of information needed to describe the outcome of a random variable Y given that the value of another random variable X is known [16] under the joint distribution

$$\pi(x, y), \quad x \in X, y \in Y$$

For the BiGAN framework the conditional entropies are defined below:

$$H^{\pi}(\boldsymbol{x}|\boldsymbol{z}) \triangleq -\mathbb{E}_{\pi(\boldsymbol{x},\boldsymbol{z})}[\log \pi(\boldsymbol{x}|\boldsymbol{z})] \tag{2.78}$$

$$H^{\pi}(\boldsymbol{z}|\boldsymbol{x}) \triangleq -\mathbb{E}_{\pi(\boldsymbol{x},\boldsymbol{z})}[\log \pi(\boldsymbol{z}|\boldsymbol{x})] \tag{2.79}$$

The Conditional entropy defined above is dependant on the underlying distribution of the random variables, in this case the distribution of the encoder and generator modules $p_G(x)$ and $p_E(z)$. In practise this value is intractable because we dont have access to the saddle points of the objective function beforehand. As an alternative, the approximation of the conditional entropy is calculated by bounding CE to the criterion of cycle-consistency [59]

Cycle consistency is the similarity of the reconstruction to the input data. Denoting the reconstruction of x as x', the cycle can be defined as:

$$x' = G(z'), \quad z' = E(x), \quad x \in \Omega_x, \quad x' \approx G(E(x)) \tag{2.80}$$

In other gan frameworks like Cycle-GAN[59], Disco-GAN [29] and Dual-GAN [56] cycle consistency constraint is implemented leveraging ℓ_k losses with $k = 1, 2$. Using ℓ_2 based pixel-wise loss functions to reconstruct the samples leads to blurry images during inference [32][35]. To enforce a better constraint and to improve the quality of the reconstructed samples, this framework suggests using the feature layer of the discriminator to compute the loss for the conditional entropy constraint. The objective function to approximate this constrainst is given below:

$$\min_{\boldsymbol{E},\boldsymbol{G}} \max_{\boldsymbol{D}} \mathcal{L}_{\text{Cycle}}(E,G,D) = \mathbb{E}_{\boldsymbol{x}\sim p_{\text{data}}(\boldsymbol{x})} \left[\log \sigma \left(f_{\boldsymbol{D}}(\boldsymbol{x},\boldsymbol{x})\right)\right] + \mathbb{E}_{\hat{\boldsymbol{x}}\sim p_{\boldsymbol{G}}(\hat{\boldsymbol{x}}|\boldsymbol{z}),\boldsymbol{z}\sim p_{\boldsymbol{E}}(\boldsymbol{z}|\boldsymbol{x})} \log \left(1 - \sigma \left(f_{\boldsymbol{D}}(\boldsymbol{x},\hat{\boldsymbol{x}})\right)\right)\right] \quad (2.81)$$

This additional adversarial training is implemented into the ALAD architecture to enforce a contraint to improve the quality of reconstructed noise and the image. Its addition is explained in the next part of the section.

2.3.3.3 ALAD Architecture

Training of the framework shares the same adversarial approach with BiGAN (2.3.2).Generator module simulataneously learns the mapping from input data to a latent representation while the encoder module learns the opposite. Model also incorporates the mentioned improvements to increase the stabilization of the training procedure. The architecture overview is illustrated in figure 26

Formally the ALAD architecture tries to match the joint distributions

$$p_E(x,z) = p_E(z|x)p_{\text{data}}(x)p_G(x,z) = p_G(x|z)p_Z(z) \quad (2.82)$$

and tries the seperate the data, noise pairs $(x, E(x))$ and $(G(z), z)$ with an adversarial discriminator module D. For this framework we refer to the main discriminator as D_{xz}. The core objective function with the updated terms is :

$$V\left(D_{xz},E,G\right) = \mathbb{E}_{x\sim p_{\text{data}}}\left[\log D_{xz}(x,E(x))\right] + \mathbb{E}_{z\sim p_Z}\left[1 - \log D_{xz}(G(z),z)\right] \quad (2.83)$$

Section 2.3.3.2 explains the convergence problem of the joint distribution. Because of the lack of constraints imposed on the p_{data} and p_Z, the objective function may not converge properly and this consequentially decreases the quality of the reconstructed samples, namely $x' \approx G(E(x))$. In

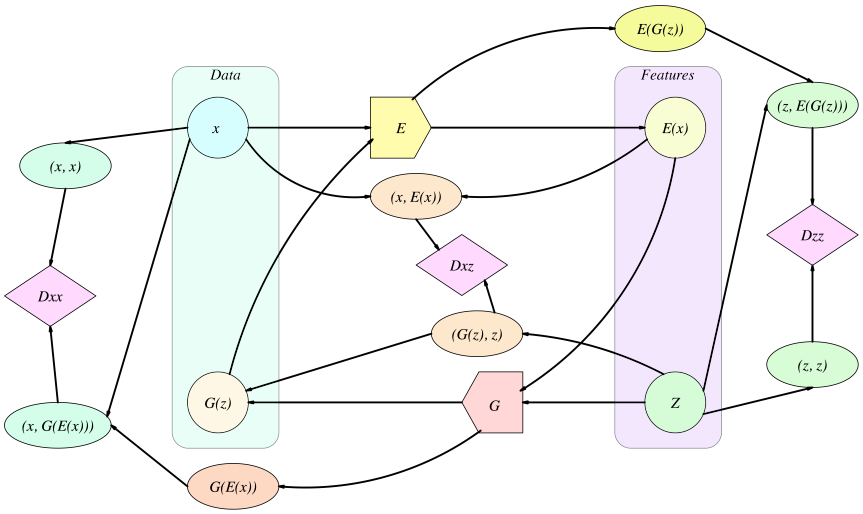

Figure 26 – ALAD architecture overview

addition to the image reconstruction, to enforce a constaint on the noise encoding from the input image, $z' \approx (E(G(z)))$, ALAD architecture also adds a second objective function to the overall adversarial training loop to regularize the conditional distributions. The CE term for the image and for the noise is defined below.

$$H^{\pi}(x|z) = -\mathbb{G}_{\pi(x,z)}[\log \pi(x|z)] \tag{2.84}$$

$$H^{\pi}(z|x) = -\mathbb{E}_{\pi(x,z)}[\log \pi(z|x)] \tag{2.85}$$

As explained in the previous section, since the saddle points beforehand can't be obtained for the computation, these terms can be approximated with the discriminators D_{xx} and D_{zz} respectively. The training of these discriminators is added to the main adversarial training loop as a part of the discriminator module training. Their objective functions are defined in equation 2.86

$$\begin{aligned} V(D_{xx}, E, G) = \mathbb{E}_{x\sim p_{\text{data}}}[\log D_{xx}(x,x)] \\ + \mathbb{E}_{x\sim p_{\text{data}}}[1 - \log D_{xx}(x, G(E(x)))] \end{aligned} \tag{2.86}$$

$$\begin{aligned} V(D_{zz}, E, G) = \mathbb{E}_{z\sim p_{\mathcal{Z}}}[\log D_{zz}(z,z)] \\ + \mathbb{E}_{z\sim p_{\mathcal{Z}}}[1 - \log D_{zz}(z, E(G(z)))] \end{aligned} \tag{2.87}$$

Putting it all together, ALAD framework solves the following combination of value function during the adversarial training.

$$\begin{aligned} &\min_{G,E} \max_{D_{xz},D_{xx},D_{zz}} V\left(D_{xz}, D_{xx}, D_{zz}, E, G\right) = \\ &V\left(D_{xz}, E, G\right) + V\left(D_{xx}, E, G\right) + V\left(D_{zz}, E, G\right) \end{aligned} \tag{2.88}$$

During the training, the generator and the encoder are updated simulatenously. In the second part of the adversarial training, all the discriminators update their weights to both regularize the reconstructions and to converge to equilibrium for the main value function. Spectral normalization is used in every convolutional layer of the discriminators. Framework also implemented them to the layers of the encoder network with the purpose of further increasing the quality of the reconstructed samples. [57].The result of the training and its analysis will be discussed in chapter 5.

The Anomaly score computation of the framework is based on the quality of the reconstructed query samples. If the reconstructed query image is distant to the original input it will obtain a greater anomaly score. ALAD framework suggests that because of the nature of the spatial data, even though there are similarities, obtained noise during reconstruction may mask potential feature similarities, preventing their detection. The suggested approach of the framework is to compute the anomaly score using the feature layer of the D_{xx} discriminator shown in equation 2.89.

$$A(x) = \|f_{xx}(x,x) - f_{xx}(x, G(E(x)))\|_1 \tag{2.89}$$

In this equation, $f(\cdot,\cdot)$ represents the vector of activations of the layer before the output of the D_{xx} discriminator [57]. Anomaly score $A(\cdot)$ captures the confidence such that the given image is well encoded and reconstructed by the generator and therefore it is from the real data distribution. [57] However different kinds of anomaly score computations are also considered for the sake of comparison.

These are (including the one discussed):

$$\begin{aligned} \bullet L_1 &: A(x) = \left\|x - x'\right\|_1 \\ \bullet L_2 &: A(x) = \left\|x - x'\right\|_2 \\ \bullet \text{ Logits } &: A(x) = \log\left(D_{xx}\left(x, x'\right)\right) \\ \bullet \text{ Features } &: A(x) = \left\|f_{xx}(x,x) - f_{xx}\left(x, x'\right)\right\|_1 \end{aligned} \tag{2.90}$$

Overall this framework aims to improve the generator and encoder learning with improvements such as spectral normalization and conditional entropy discriminators. Its performance with our dataset and ways to improve the adversarial training will be discussed in chapter 5

2.3.4 GANomaly & Skip-GANomaly

GANomaly framework [2] and Skip-GANomaly [3] are the most recent models that focuses on the anomaly detection using adversarial training. Their performance on the benchmark datasets like CIFAR-10 [31] and SVHN [40] exceeds the previous mentioned frameworks. This section will explain their structure and their differences in terms of one another.

GANomaly and Skip-Ganomaly models differ with a significant change in the model itself. Both models contain a generator and discriminator modules but generator module is actually composed of an adversarial autoencoder network. Details of the both architecture will be discussed in order.

Generator module of the GANomaly framework composed of an encoder-decoder network as can be seen in figure 27. The third module is the encoder network for the generated samples. Generator network takes the image data as an input and sequentially it creates the latent representation of the image and reconstruction from the latent representation then the second encoder network encodes the latent representation of the reconstructed sample. Discriminator network shares the same functionality as in GAN framework. [23]

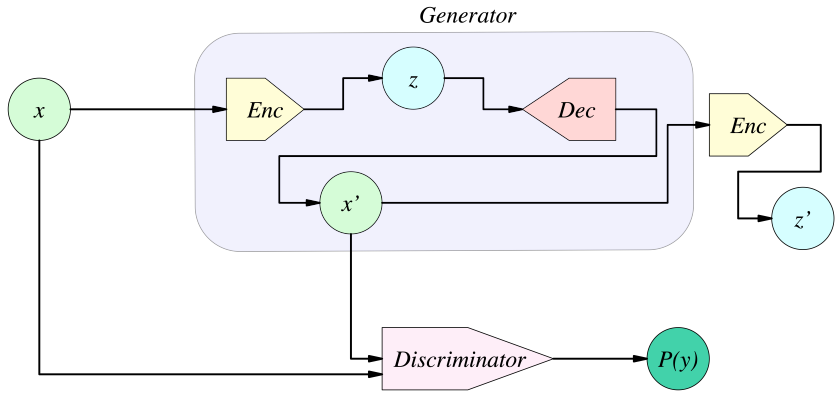

Figure 27 – GANomaly architecture overview

With the use of the adversarial autoencoders, framework obtains a superior reconstruction ability compared to the previous models. But in doing so, its generative sub-module decoder is not a true generative component from the perspective of the generative adversarial networks. With the change of the model architecture its training objective also changes. GANomaly framework uses adversarial training scheme but its generator module loss is the combination of 3 separate loss functions. These are:

- Adversarial Loss
- Contextual Loss
- Encoder Loss

Adversarial loss represents the loss function component for the adversarial training of the framework. Instead of maximizing the probability of discriminator's attaining generated image as real, it has a loss function derived from the [48] that uses feature matching. The main purpose of this type of loss function is to reduce the instability in the GAN training. Adversarial loss depicted in equation 2.91 is the $\mathcal{L}_2$ distance of the feature representation of the original and the generated image, respectively. [2] Feature layer is extracted from the activation layer before the output of the discriminator.

$$\mathcal{L}_{adv} = \mathbb{E}_{x \sim p_{\mathbf{x}}} \| f(x) - \mathbb{E}_{x \sim p_{\mathbf{x}}} f\left(G(x)\right) \|_2 \tag{2.91}$$

Only adversarial loss does not help to optimize the generator towards reconstructing images similar to the input data. To this end, contextual loss is also added to the generator loss function. According to [26], using $\mathcal{L}_1$ instead of $\mathcal{L}_2$ decreases the blurriness in the generated images, so the following contextual loss that measures the distance between original image and the generated one is added to the to the total generator loss.

$$\mathcal{L}_{con} = \mathbb{E}_{x \sim p_{\mathbf{X}}} \| x - G(x) \|_1 \tag{2.92}$$

Additional encoder loss is also added to the generator to improve the encoding of the latent representation of the reconstruction. This loss function aims to minimize the distance between the encoded latent representation of the input image and the reconstruction. The Loss function is depicted below.

$$\mathcal{L}_{enc} = \mathbb{E}_{x \sim p_{\mathbf{X}}} \| G_E(x) - E(G(x)) \|_2 \tag{2.93}$$

Overall, the objective loss function of the generator is defined in equation 2.94 where the weight parameters w_{adv}, w_{con} and w_{enc} are used to change

the impact of individual losses.

$$\mathcal{L} = w_{adv}\mathcal{L}_{adv} + w_{con}\mathcal{L}_{con} + w_{enc}\mathcal{L}_{enc} \tag{2.94}$$

GANomaly framework uses encoder loss function also as an anomaly score measure.

$$\mathcal{A}(\hat{x}) = \|G_E(\hat{x}) - E(G(\hat{x}))\|_1 \tag{2.95}$$

Skip-GANomaly framework[3] is the continuation of the GANomaly architecture with changes mainly to the generator network. As can be seen from figure 28, encoder and decoder networks inside the generator framework is connected using skip connections.

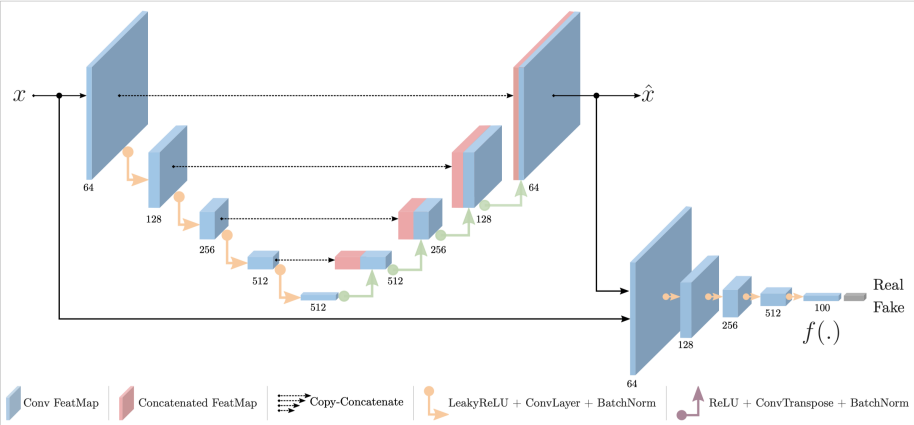

Figure 28 – Skip GANomaly architecture overview [3]

At each layer of the encoder, convolutional feature map is concatenated to the corresponding decoder layer. Addition of skip connections provides a better reconstruction capability to the generator than the GANomaly framework. [2]. Generator objective function is built using the same logic. Because of the exclusion of the secondary encoder network, the encoder loss is obtained using the feature layer of the discriminator.

$$\mathcal{L}_{enc} = \mathop{\mathbb{E}}_{x \sim p_x} |f(x) - f(\hat{x})|_2 \tag{2.96}$$

To find anomalies during the inference stage, Skip-GANomaly framework combines the encoder loss with the use of contextual loss.

$$\mathcal{A}(\dot{x}) = \lambda R(\dot{x}) + (1 - \lambda)L(\dot{x}) \tag{2.97}$$

$R(\dot{x})$ represents the contextual loss with the reconstruction term and $L(\dot{x})$ represents the encoder loss with the latent representation term. Term λ is used to adjust the impact of the loss functions to the overall anomaly score.

Both GANomaly and Skip-GANomaly uses adversarial encoder architecture in their generator networks and therefore have superior reconstruction capabilities compared to the previous 3 framework. The primal problem with their architecture is that they don't adapt the true distribution of the input data. They learn the underlying latent representation well to reconstruct the input and detect anomalies. However their generator network represents the scenerio where the generator has learnt the input data distribution fairly well. In order to improve the results of a GAN based anomaly detection framework, insights gained from these 2 networks are significantly important. Their contribution to the improved framework and their performance analysis regards to other models will be explored in chapters 4 and 5 respectively.

CHAPTER 3

Latest Developments

This chapter presents the developments in the field of anomaly detection and generative adversarial networks. Although the models mentioned in the state of the art chapter deliver certain level of performance, potential improvements are still a possibility. These improvements are related to both adversarial training of the generator and discriminator networks and different strategy to stabilize the training of encoder network present in the overall framework. In the following sections, some of these improvements that are later adopted by our framework will be introduced and their contribution to solve the disadvantages we observed in the previous frameworks will be discussed.

3.1 F-AnoGAN Framework

AnoGAN [50] is considered as the first framework that uses generative adversarial networks for an anomaly detection task. The main problems with this framework, are the stabilization issues of the adversarial training, and the second stage of the framework which was mapping from the latent representation to the input data distribution which can be also considered as the inverse mapping of the generator. The model used back propagation to approximate the latent representation for every query image to compute the anomaly score which resulted a very poor performance in terms of the computation time. This was the main disadvantage of the framework because it is very challenging to integrate into a real life application with an implausible inference time. F-AnoGAN (Fast AnoGAN) framework [49] aims to eliminate this issue by implementing a new training strategy. It

also uses a new objective function for the adversarial training to further stabilize the generator discriminator performance. In the rest of the section, F-AnoGAN framework, its training strategies and anomaly detection methods will be discussed.

The framework architecture of F-AnoGAN is very similar to the BiGAN [17] framework. It consists of a generator discriminator for the adversarial learning and an encoder network to learn the inverse mapping from latent representation to the input image data.

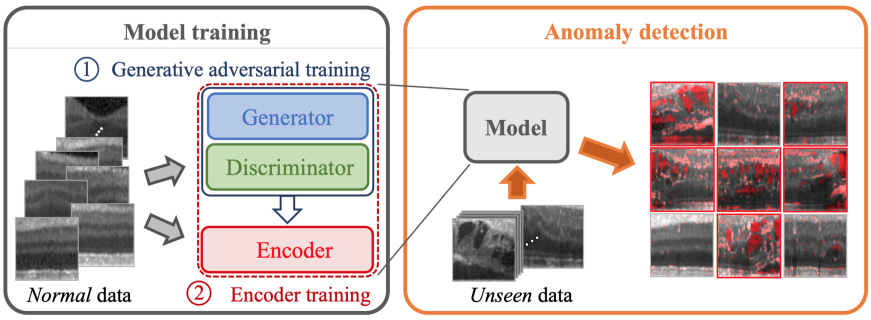

Figure 31 – F-AnoGAN Framework Overview [49]

The first improvement is the change of the training style of the whole framework. In BiGAN approach, encoder and generator is trained simultaneously to fool the discriminator. Hence discriminator is modified to classify the pairs of noise (latent representation) and images instead of the single image approach used in the GAN framework. Therefore it tries to distinguish samples from a joint distribution which explained in section 2.3.2. Including encoder to the adversarial setup also introduces instability issues which ALAD Framework [57] tried to mitigate with additional discriminators that approaximate conditional entropy. (section 2.3.3.2). F-AnoGAN framework addresses this issue by seperating the training of the encoder from the generator discriminator pair. The new framework can be seen in figure 32.

This new training scheme comprises of the stages. In the first stage GAN framework is trained. The objective function for the adversarial training is also replaced with the Wasserstein GAN's objective function [7] although training of the GAN can be performed with any other framework's approach (including the original GAN framework) according to the [49].

In the second stage, encoder network is trained using generator and discriminator with locked weight. Two seperate pipelines are used to measure

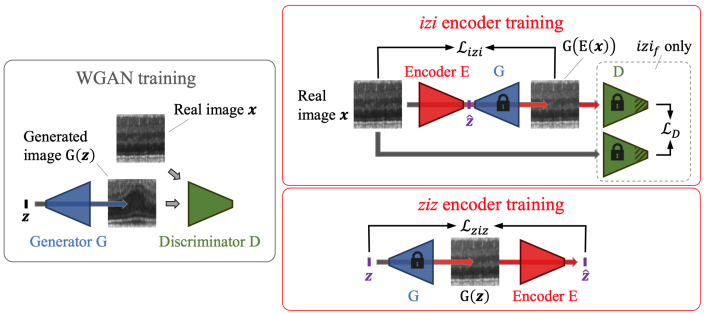

Figure 32 – F-AnoGAN Training Strategies [49]

the performance of the encoder. These are izi (image-noise-image) and ziz (noise-image-noise) respectively.

IZI Encoder Training

IZI method follows the standard autoencoder network approach. The generator network with fixed weights acts as a decoder network. During the training, same image dataset used in the first stage for training gan is mapped to a latent mapping z by a trainable encoder and then reconstructed using the fixed generator network. Training objective for this setup is to minimize MSE (Mean Squared Error) based reconstruction error of the input image x and the reconstructed image $G(E(x))$.

$$\mathcal{L}_{izi}(\mathbf{x}) = \frac{1}{n}\|\mathbf{x} - G(E(\mathbf{x}))\|^2 \tag{3.1}$$

This approach has an important drawback regarding to latent representation. Since the distribution of the latent representation of the input image is not known, the encoder is trained only using a form of contextual loss which enforce the similarity only in the image space. Without the insufficient information about the latent space, encoder may map images to a representations such that the reconstructions are not convincing enough for the discriminator to evaluate as real. [49]. Therefore the framework suggests also including a latent space based loss function derived from the feature layer of the discriminator to guide the encoder training. Improved izi_f training objective is defined below.

$$\mathcal{L}_{izi_f}(\mathbf{x}) = \frac{1}{n} \cdot \|\mathbf{x} - G(E(\mathbf{x}))\|^2 + \frac{\kappa}{n_d} \cdot \|f(\mathbf{x}) - f(G(E(\mathbf{x})))\|^2 \tag{3.2}$$

where the $f(\cdot)$ represents the feature layer of the discriminator as a statistics, n_d is the dimensionality of the intermediate feature representation f and κ denotes the weighting factor for the inclusion of the discriminator guidance.

ZIZ Encoder Training

Different from the IZI method, this approach reverses the auto encoder setup and forms a decoder encoder architecture. A random sampled noise from the z-space is mapped to the image space using the fixed generator and then generated sample is encoded using the trainable encoder network. The loss for the training is defined as the MSE based reconstruction of the noise which depicted in equation below.

$$\mathcal{L}_{ziz}(\mathbf{z}) = \frac{1}{d}\|\mathbf{z} - E(G(\mathbf{z}))\|^2 \tag{3.3}$$

The shortcoming of this approach is that even though the encoder is trained with a loss that will enforce a similarity in latent space, encoder sees only images that are generated by the generator. It doesn't see any image samples from the training dataset which affects the contextual similarity of the reconstruction of learned latent space distribution.

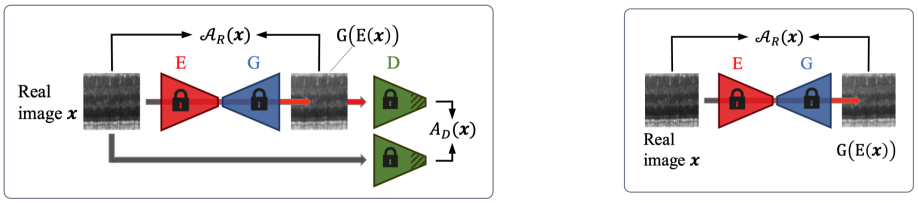

(a) Anomaly Score computation scheme for izi and izi_f method

(b) Anomaly Score computation scheme for ziz architecture

Figure 33 – Anomaly Score computations for both training methods [49]

To calculate the anomaly score for inference, deviation of the query images from their reconstructions are quantified. Figure 33 represents the anomaly score computations for both training methods.

IZI_f method uses the same loss functions for the computation of the anomaly score. Anomaly score for image x is defined as:

$$\mathcal{A}(\mathbf{x}) = \mathcal{A}_R(\mathbf{x}) + \kappa \cdot \mathcal{A}_D(\mathbf{x}) \tag{3.4}$$

$$\mathcal{A}_R(\mathbf{x}) = \frac{1}{n} \cdot \|\mathbf{x} - G(E(\mathbf{x}))\|^2 \tag{3.5}$$

$$\mathcal{A}_D(\mathbf{x}) = \frac{1}{n_d} \cdot \|f(\mathbf{x}) - f(G(E(\mathbf{x})))\|^2 \tag{3.6}$$

For IZI and ZIZ method, the computation of the anomaly score reduces down to $\mathcal{A}_R(\mathbf{x})$ function only. Both training methods yields a similar anomaly score computation for the anomalous samples. Since the models are trained with a dataset that doesn't contain any anomalies, the query images that have anomalous regions results in poorer reconstruction hence a higher anomaly score while the normal images produce a more similar reconstructions to the original sample.

The Significance of this framework is that it separates the training of the encoder from the adversarial setting of the GAN's while preserving the inverse mapping functionality for the inference. Chapter 4 will explain its contribution to the proposed improved framework.

3.2 Energy Based Generative Adversarial Networks

Training a GAN framework perhaps the most sensitive part of working with them. There has been an extensive amount of research to improve the stabilization of the adversarial training or perhaps offer a new methodology. [48] and [6] offer number modifications to the original adversarial training setup to improve the generation performance ,increase the stabilization and prevent issues such as mode collapse[1]. [7] and [24] offers a new method to compute the loss and ways to stabilize it. Mainly because of its adversarial setting, training of GAN frameworks will always be a topic of interest. Energy based generative adversarial networks [58] offers a new training method by redefining the loss functions and the functionality of the discriminator network. This section will introduce the architecture and how it works.

Energy based models measures the current state of the model by assigning a scalar predefined energy as a degree of compatibility [33]. Training

[1]Mode collapse is the scenerio where generator learns enough information to fool the discriminator very early. It finds a generation that fools the discriminator and does not learn anything else from the discriminator. Because of that all the generated samples from the generator look the same, defeating the purpose of generating from the distribution of the data.[6]

energy based models consists of mapping low energy outputs to the samples with the "correct" class, and mapping higher energy outputs to the "incorrect" class. From the perspective of GANs, EBGAN model is trained to ouput lower energy for the real data, while the generated data (fake images) outputs a higher energy. The model architecture can be seen in figure 34.

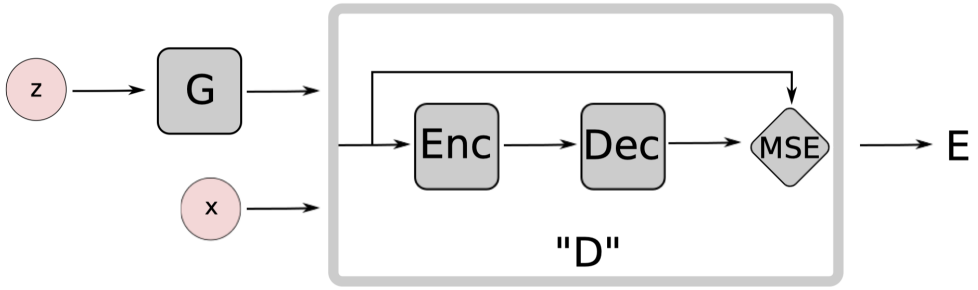

Figure 34 – EBGAN Model Structure [58]

The main structural difference of this framework from the other ones is that discriminator is defined as an auto encoder network to provide the reconstruction of the inputs. The energy value function is defined as the margin loss of the input and the reconstructed sample [58] as a reconstruction error.

Formally a margin is used to create an energy gap between the correct output and the incorrect output. For data sample x, and a generated sample $G(z)$ with z being sampled from a known distribution p_z, The discriminator loss $\mathcal{L}_D$ and the generator loss $\mathcal{L}_G$ are formally defined in equation 3.7.

$$\begin{aligned} D(x) &= \|\,\mathrm{Dec}(Enc(x)) - x\| \\ \mathcal{L}_D(x,z) &= D(x) + [m - D(G(z))]^+ \\ \mathcal{L}_G(z) &= D(G(z)) \end{aligned} \tag{3.7}$$

where $D(x)$ is the reconstuction loss and $[\cdot]^+ = \max(0,\cdot)$. Minimizing $\mathcal{L}_G$ with respect to the generator is similar to maximizing the second term of the $\mathcal{L}_D$. Instead of calculating the probability of the input being real or fake, discriminator is responsible for attaining the correct amount of energy to the input images.

Using autoencoder network as a discriminator brings additional advantages to the training setting. Rather than using a single target information

to train the model, reconstruction based output offers a more diverse targets for the discriminator [58]. One of the reasons of the stabilization issues in the adversarial training is that discriminator might provide gradients not useful enough for generator to improve the quality of the generated samples. Having a reconstruction loss output might provide a better gradient in terms of different directions as opposed to binary logistic loss[58]. Another advantage is that even though they are trained with an adversarial setting, autoencoder networks might prove useful to learn the underlying energy manifold of the data without supervision or negative examples when they are trained using a proper regularization constraint. This means that in this setting generated samples and input data are both used to model the underlying energy manifold of the data.

EBGAN framework argues that, the discriminator network is regularized by exposing generated samples from the generator which it should output higher reconstruction energies [58]. The benefit of this regularization is that instead of a hand crafted predefined one, the regularization term can also be trained along with the discriminator. Adversarial training allows a direct connection between learning the energy function and producing contradictive samples in that regard.

EBGAN framework also adds additional penalty called pulling away term (PT) that run at a representation level to prevent mode collapse depicted in equation 3.8.

$$f_{PT}(S) = \frac{1}{N(N-1)} \sum_{i} \sum_{j \neq i} \left(\frac{S_i^\top S_j}{\|S_i\| \, \|S_j\|} \right)^2 \tag{3.8}$$

S is the feature output from the encoder for generated images. Pulling-away term measures the cosine similarity among all generated images features S in a minibatch. If the mode collapses, the feature vectors will thereupon be similar, i.e. the angles are close to zero and the cosine will max-out. Therefore, it will add a high penalty if there are too similar. [58]

EBGAN framework offers a more flexible approach to train the discriminator and generator network. Transition from convolutional based discriminator to autoencoder network also provides a potential inclusion for the computation of the anomaly score. Its impact on the proposed framework will be discussed in the next chapter.

CHAPTER 4

Architectural Improvements

This chapter presents the modifications applied to aforementioned approaches to improve the performance of the anomaly detection. All the discussed models measures its performance metric on well known datasets, such as CIFAR-10 [31] and SVHN [40]. The dataset used in this thesis presents additional challenges to this problem we aim to solve. The first section will introduce its dataset to the reader and will give examples. Next section will discuss the shortcomings of the previous approaches regarding the interpretation of the dataset and detection of the existent anomalies. Sections 4.2.3 and 4.3 will explain the modified architecture and the significance of the changes.

4.1 SEM Image Dataset

Nanofibrous materials acquired increasingly significant demand from variety of fields in the Industry. It constitutes a foundation material for a lot of products including areas in medicine, filtration, sensors and manufacturing applications. [12]. Despite the demand and continuous research development towards its production, manufacturing nanofibrous materials is still challenge for scaled of mass production. Several techniques for producing nanofibers have been presented in the literature. [12]. Electrospinning method is the focus of this anomaly detection task. It produces a structure which consists of filaments woven in with randomized geometric pattern. You can see one of the images of the material produced without any anomalies in figure 41.

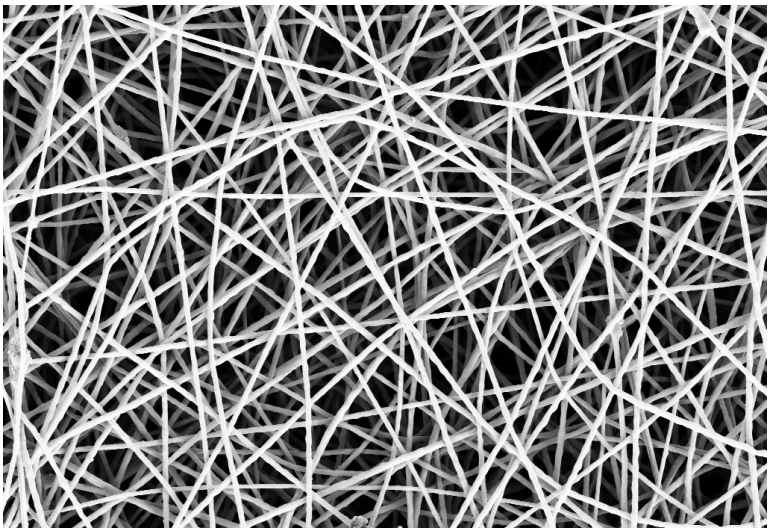

Figure 41 – Part of Training Dataset from the SEM Image Dataset [51]

Dataset consists of 5 images with no anomalies and 40 sample images that have various types of anomalous regions. To preserve computational efficiency without sacrifising from performance, training dataset and testing dataset is sampled from SEM image dataset.

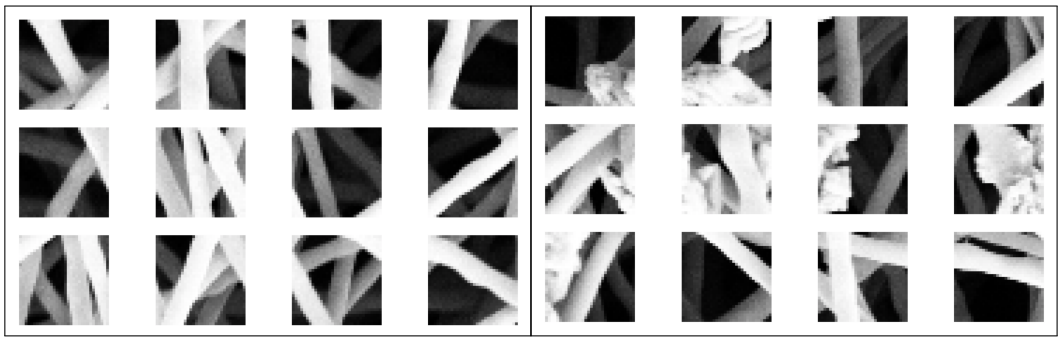

(a) Normal regions **(b)** Anomalous regions

Figure 42 – Normal and Anomalous region patches for the training and testing

32×32 patches are selected as the image size as if proposed framework prove useful for the anomaly detection, testing the model with other known datasets such as CIFAR10 [31] and SVHN [40] would be more con-

venient. 28×28 patch size is also considered but choosing 28×28 image size forced model to have less transposed convolution layers (see chapter A for model details) and GAN models designed with that architecture experienced model collapse frequently in the preliminary experiments. Figure 42a shows the example patches used for the training phase. Training dataset consists of patches which contains no anomalies. Figure 42b shows the anomalous samples which are used in the inference stage. The Anomalous regions can reside in both the topmost layer or can be hidden in deep in the woven structure.

4.2 Analysis of Aforementioned Approaches

This section presents an analysis on the performance of GAN based state of the art anomaly detection methods presented in section 2.3 and a discussion to identify the shortcomings of these methods. Stabilization issues in the adversarial training stage, reconstruction problems related to the encoding of latent representation and the method of computing the anomaly score will be discussed. While discussing these issues, the proposed model will be introduced incrementally by addressing the modifications and measures to mitigate the affect of these shortcomings to the performance.

Proposed methods in chapter 2 can be further divided into 2 seperate categories with respect to their generator structure.

- Pure GAN (AnoGAN (2.3.1), BiGAN (2.3.2) and ALAD (2.3.3))
- Autoencoder Variants (GANomaly and Skip-GANomaly (2.3.4))

First group has a generator that accepts the noise as an input and uses adversarial training to match the generated sample distribution to the input data distribution. The latter uses an autoencoder based decoder in favor of the generator but still employs adversarial training to learn the latent representation. During the analysis of the first two observations, autoencoder variants will not be considered for discussion since their generator network does not suffer from the stabilization issues of GANs.

4.2.1 Stabilization of Adversarial Training

Generator and discriminator's objective function stabilization is still an important issue in GAN training. Various approaches and modifications are experimented to further improve the training of the GANs and prevent non convergent scenerios. [6] and [48] proposed additional stabilization "tricks" to improve the convergence properties of the objective function and prevent

mode collapse. These include adding noise with a decay over time to both input image and generated sample before putting through discriminator to add a factor of robustness to the discriminator, using soft labels to define the true and fake member class instead of the binary truth values and flipping labels of the true and generated images to fool the discriminator even more and provide higher gradient flow to generator early on in the training to help it learn to generate images better [48].

In the training phase of an generative adversarial network, loss values of generator does not portray a traditional convergence line in plots. Adversarial minimax game prevents the losses of the player networks to converge to a certain limit. If the loss is reaching zero in any case, it indicates a problem in the learning capacity of one of the networks. If discriminator loss converges to zero too quickly, it means that it learned to discriminate between the real images and the ones generated by the generator network. On the other hand if the generator loss converges to zero early in the training it indicates a mode collapse but situation may arise in even normal looking training sessions. The problem is at some point in the training generator generates an image that perfectly fools the discriminator. If gradients obtained from this loss computation is high enough, generator might stop learning from the gradient flow of discriminator and start to generate the same sample in each iteration. This sample also may not be visually similar to the target distribution. This eliminates the purpose of having a generator network.

To mitigate these shortcomings, ablation study is performed on all Pure GAN models which consists of previously mentioned training improvements with same model capacity and training hyperparameters to create an equal environment for the models. Despite models proving a certain performance standard on the benchmark datasets ([31, 40]), they performed poorly on the SEM image dataset ([51]). More importantly, the training of the networks were unstable enough to prevent to obtain a consistent performance benchmark. Obtaining a stable GAN for generating reconstructions is fairly important because it is the first step of the anomaly detection framework. Figure 43 presents the generator/discriminator learning graphs and their generation samples from the final training epoch.

As seen in the figure, discriminator is gradually learning to differentiate between the real and generated image while the generator network does not seem to set its loss to a certain level as desired. This trend is observed in the majority of the experiments and in the ablation study as well. From the perspective of the image generation, samples generated from GANs are not

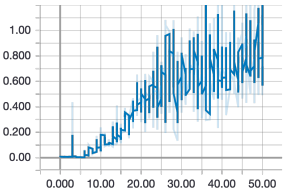

(a) AnoGAN generator training

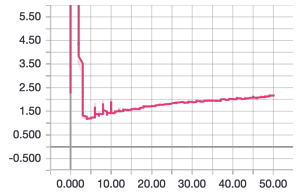

(b) BiGAN generator training

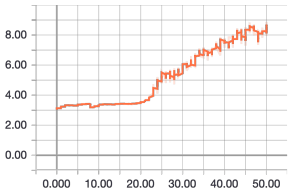

(c) ALAD generator training

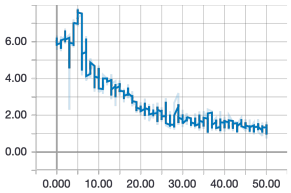

(d) AnoGAN discriminator training

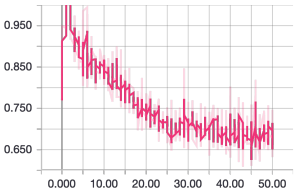

(e) BiGAN discriminator training

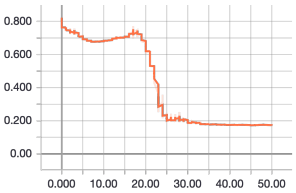

(f) ALAD discriminator training

(g) AnoGAN generated image sample

(h) BiGAN generated image sample

(i) ALAD generated image sample

Figure 43 – Training information for the Pure GAN models. For graphs, x axis is the number of epochs and the y axis is the loss value

contextually sound enough to represent the target distribution of the SEM image dataset. To obtain a more concise observation the reconstructions of these GANs will also be inspected.

$$\begin{aligned} D(x) &= \|\,\mathrm{Dec}(Enc(x)) - x\| \\ V(G,D) &= D(G(z)) + D(x) + [m - D(G(z))]^+ \\ \mathcal{L}_D(x,z) &= D(x) + [m - D(G(z))]^+ \\ \mathcal{L}_G(z) &= D(G(z)) \end{aligned} \tag{4.1}$$

Considering the results of these experiments, training objective of the EBGAN

model is adopted to obtain a more stable training with our dataset. (See eqn. 4.1)

Defining loss function as a value of energy still preserves the adversarial aspect of the objective function. An auto encoder network acts as a discriminator module and attains an energies to the real and fake image samples with high energy values assigned to generated images. Generator tries to "fool" the discriminator to decrease the amount of energy fake image is assigned. Here the energy term is described as the ability of discriminator to reconsturct the given output, so it is a reconstruction error based value.

Using energy based GAN proved useful to obtain a consistent performance without having issues with argued stabilization problems. Details regards to its training and model's reconstruction capability will be discussed in its own section.

4.2.2 Convergence of Encoder Training

Stabilizing the GAN training is actually the second step for a reconstruction based anomaly detection approach. As proposed, generator network learns the mapping from the latent space Z to the image space X. However in order to test unknown images for anomalies, the latent representation of the image must be extracted. From this point on this operation is called the "inverse mapping". Generators are not able to provide this kind of inverse mapping so pure gan based models followed different approaches to obtain this information.

AnoGAN model implements a backpropagation routine for a predetermined number of steps to approximate the latent representation of the query image. It randomly initializes a latent representation vector and updates it until the loss that is defined as the ℓ_2 norm of the query image and generated sample converges. The main disadvantage of this approach is the time constraint. Method works with image patches so processing whole image takes a considerable amount of time compared to other methods.

BiGAN and ALAD on the other hand, adds an additional encoder network to their adversarial training to learn the inverse mapping while learning the image distribution (see eqn. 4.2).

$$\begin{aligned} V(D,E,G) = &\mathbb{E}_{x\sim p_{\text{data}}}\left[\log D_{xz}(x,E(x))\right] \\ &+ \mathbb{E}_{z\sim p_Z}\left[1-\log D_{xz}(G(z),z)\right] \end{aligned} \tag{4.2}$$

To learn both mappings, models learn the joint probability distribu-

tion of the image and the noise pairs. Discriminator network therefore is modified to process this new representation (see implementation details in appendix A.2 and A.3). Integrating an encoder network solves the time constraint problem because the latent representation is acquired with feeding the query image to the encoder network at the inference stage and the computation time is negligible compared to AnoGAN's approximantion. Nonetheless addition of a new component to the adversarial training brings new stabilization problems with regards to encoder network. Training of the generator discriminator, implicitly affects the quality of the representation encoded. ALAD implements additional discriminators to control the conditional probability distributions of the learned joint distribution from both ends (For noise and for image) to improve the encoder performance but experiments did not provide a considerable advance even with ablation study. Figure 44 presents the training graphs of the models and their obtained reconstructions. AnoGAN model does not have a training graph for encoder since it uses a backpropagation and it would have a convergence graph for each patch in the dataset. Instead, the training graph of the first iteration of the proposed model's encoder is presented.

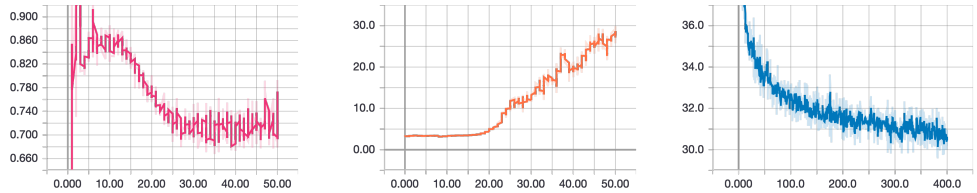

(a) BiGAN Encoder Training

(b) ALAD Encoder Training

(c) ENCEBGAN Encoder Training

Figure 44 – Training graphs of pure GAN models that implement encoder network and the first iteration of the proposed network

By itself, these training graphs does not give us a reliable insight about encoder performance. Other than its quantative results, encoder networks performance can be quantified with models' ability to reconstruct a given image after training. At this point in pipeline, impact of a good generator also comes into play. In both models, the training of the encoder network is computed by feeding the latent representation obtained from the encoder and feeding it to the generator to reconstruct the training data. So performance and proper training of the encoder network also depends on the adversarial training of generator. In the minimax game played by BiGAN and ALAD, both encoder and generator tries to fool the discriminator. Therefore stabilization problem of generator inadvertantly affects

the encoder convergence which also affects the quality of the reconstructions obtained from the model. Some distortions and the information loss is expected in the generator based reconstruction. In our dataset, these imperfections cause reconstructed samples to be interpreted as anomalous sample though the input is a normal sample. Figure 45 shows the reconstructions from AnoGAN, BiGAN and ALAD's inference stage.

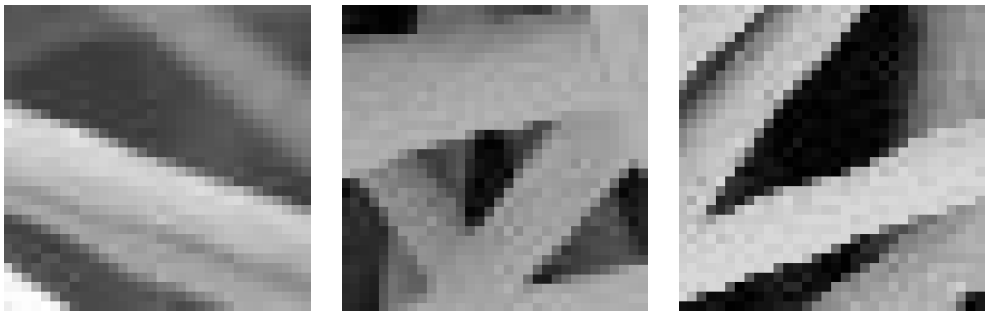

(a) AnoGAN Query Image

(b) BiGAN Query Image

(c) ALAD Query Image

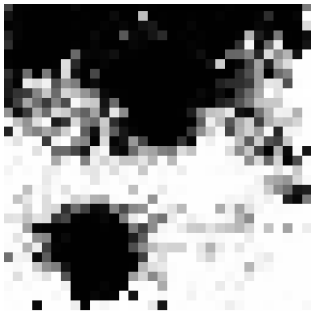

(d) AnoGAN Reconstruction

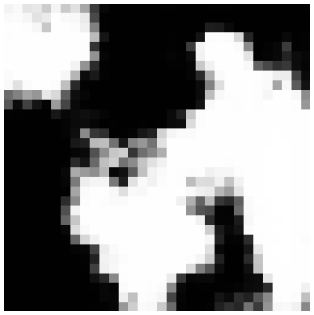

(e) BiGAN Reconstruction

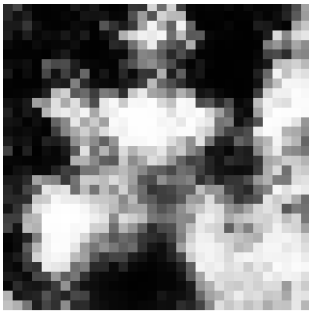

(f) ALAD Reconstruction

Figure 45 – Reconstructed samples from the pure GAN models. Upper row is the given query image and the bottom row is their reconstructions

Proposed model in this work also uses additional encoder network to get the inverse mapping information. Several modifications are applied to the training in order to improve the stabilization and ensure the convergence of the encoder. Eqn. 4.1 propose the modified generator discriminator approach. Addition of the encoder network and its training is also based

on an energy based training.

$$\begin{aligned} D(x) &= \|\operatorname{Dec}(Enc(x)) - x\| \\ V(G,E,D) &= D(G(z)) + D(x) + [m - D(G(z))]^{+} + D(G(E(x))) \\ \mathcal{L}_E(x) &= D(G(E(x))) \end{aligned} \tag{4.3}$$

Like AnoGAN and ALAD, proposed model also trains encoder network with generator networks help to obtain the reconstruction. However, instead of training all the networks in the adversarial setting, proposed model separates the trainig of the generator discriminator pair and the encoder network. Training strategy presented in F-AnoGAN framework (see section 3.1) proposes an initial adversarial training. In the second part of the training the encoder network is trained by creating a pipeline with the other network components with fixed weights (inference mode) (See figure 32). This approach focuses on the encoder training objective by removing the dependency between encoder and generator which in turn also decreases the potential stabilization issues of the generator network.

So far, configuring the models' objective function to an energy based setting and separating the joint training into sequential steps give the model two opportunities:

- The stabilization of the GAN training, which means better reconstruction performance.
- Easy convergence for encoder network because it isn't trained concurrently with the generator so learning latent reprensetation is uni directional gradient descent.

Next section will discussed the model with the mentioned changes and continue to analyze the existent shortcomings despite the improvements.

4.2.3 Encoded Energy Based Generative Adversarial Network

The first iteration of the proposed model is called encoded energy based generative adversarial network,or ENCEBGAN. This section presents how its built, its training scheme and the issues it solved.

ENCEBGAN consists of an energy based generative adversarial network framework with an additional encoder network. The roles of the networks are identical to BiGAN (2.3.2). Two main differences are the change in

the rationale in adversarial training component and separation of the encoder network training. Figure 46 presents the network components with an emphasis on the training sequence.

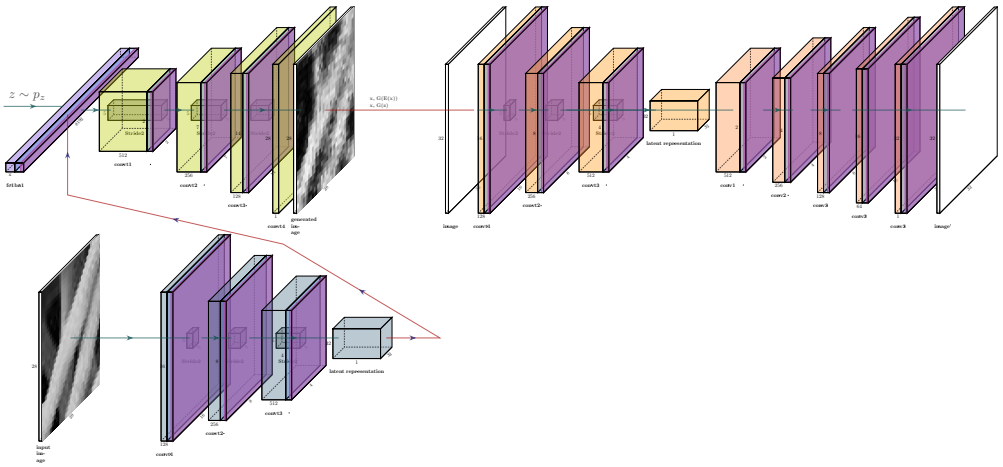

Figure 46 – ENCEBGAN Model Overview

Training of the model is divided into two sections. In the first section generator and discriminator trains adversarially to learn the mapping from image space to latent space. While generator learns the mapping, discriminator is concurrently learning to reconstruct the training dataset and learns to encode the training data on its own. This latent representation will be used later on as an auxilary information for anomaly score computation. After the adversarial training is completed, pipeline is created from the encoder generator networks to form a conceptual autoencoder and whole network is trained using the reconstruction error based objective function for the encoder network. In second stage, generator and discriminator don't learn any additional information about the dataset. This approach proved to be useful to stabilize both generator and encoder hence increased the reconstruction quality of our model. Anomaly score computation is the same as the pure gan based methods which is the reconstruction error between the query and the output of encoder generator pipeline as depicted in equation 4.4.

$$\mathcal{A}(x) = \|x - G(E(x))\|^2 \tag{4.4}$$

Figure 47 presents the training graph information and reconstructed samples as a comparison to reconstructions in figure 45.

With previously mentioned architectural improvements, ENCEBGAN performed better than BiGAN and ALAD and obtained the same perfor-

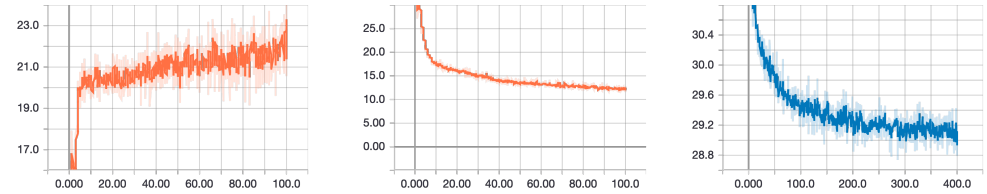

(a) Generator Training Graph

(b) Discriminator Training Graph

(c) Encoder Training Graph

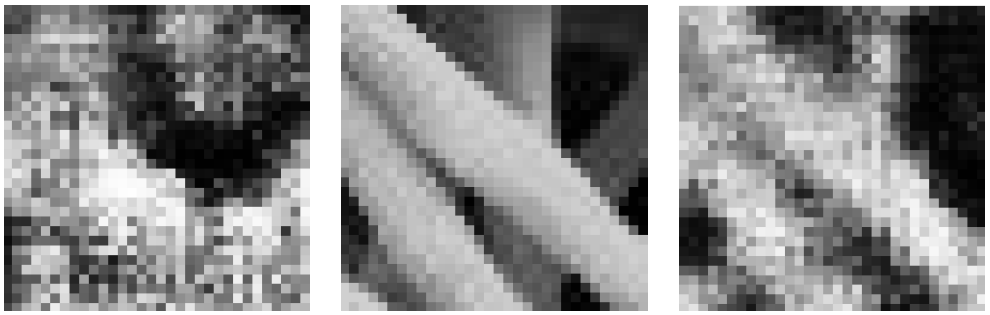

(d) ENCEBGAN Generated Sample

(e) ENCEBGAN Query Sample

(f) ENCEBGAN Reconstruction

Figure 47 – Training graphs and qualitative examples from ENCEBGAN Model

mance as AnoGAN which will discussed in chapter 5. Seperating the training of encoder and changing the adversarial objective function mechanics consequently stabilized the convergence of both networks and the reconstruction quality has increased compared to the pure gan based models.

Imperfections in the reconstructions are usually expected in reconstruction based anomaly detection methods since the network trained to learn the latent representation is regularized to prevent overfitting. In SEM image dataset, anomalous regions can occur in any level of the image with varying levels of brightness. During the experiments of the models it is observed that, imperfections in the reconstructions may be identified as anomalous regions even though the image is anomaly free. This issue inadvertently cripples the anomaly detection performance of ENCEBGAN (and other pure gan based models).

Next section will discuss the anomaly score computation methods featured in both pure gan based and autoencoder variant models, and explan the addition of a secondary encoder network to improve the overall performance of the proposed model.

4.2.4 Anomaly Score Computation

Previously we divided the state of the art gan based anomaly detection methods into two main categories. Pure gan based models and autoencoder variants. The main difference between these groups is that decoder (generator equivalent) network of these models is trained only with the latent representation of the image supplied from the encoder network. Since they learn to reconstruct using the encoded version of the training data, their reconstructions are superior compared to the pure gan based methods. Figure 48 shows an example reconstruction from both GANomaly and Skip-GANomaly 2.3.4.

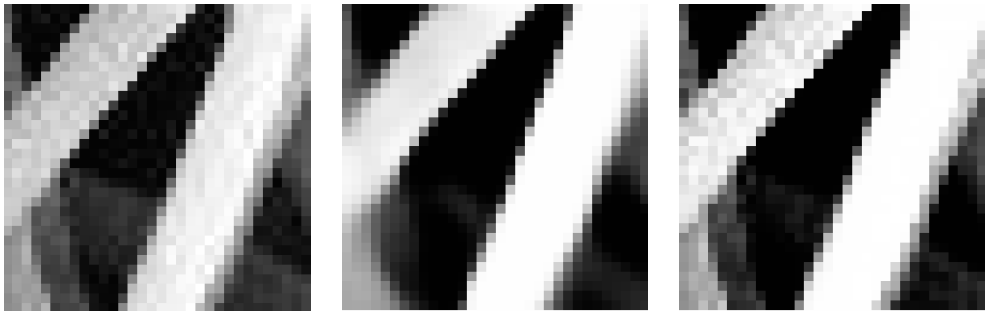

(a) Query Sample

(b) GANomaly Reconstruction

(c) Skip-GANomaly Reconstruction

Figure 48 – Reconstruction examples of Autoencoder Variant Models

Architectural difference between GANomaly and Skip-GANomaly is the additional skip connections between the encoder and decoder network of the latter. This information transfer enables Skip-GANomaly to retain more information about the data and help it to accumulate this data across the layers during the decoding stage of the reconstruction. One interesting observation is that even though the general quality of the Skip-GANomaly model is better than GANomaly on the SEM image dataset, ablation study performed in chapter 5(see Table 54 and 55) shows that overall GANomalyprediction performance is superior compared to Skip-GANomaly.

Both anomaly score computation is based on the reconstruction based error, but GANomaly uses a secondary encoder network to learn the latent representation of the reconstruction and uses this information to compute the anomaly score (see eqn. 2.95). Skip-GANomaly on the other hand composes the contextual data (reconstruction loss) with the latent loss which is obtained from the feature layer of its discriminator network (see eqn. 2.97). We speculate that training a secondary encoder network improved

GANomaly model's interpretation of the anomalous sample data. Erroneous predictions that are caused due to misinterpreting imperfect reconstructions as samples that contains anomalous regions may be averted by interpreting both input image and its reconstruction at the latent dimensional complexity.

Considering these observations and related improvements, next section will present the final version of the proposed model for anomaly detection. General architecture of the model, its training procedure and its inference stage for anomaly detection will be discussed.

4.3 Sequentially Encoded Energy Based Generative Adversarial Network

Sequentially encoded energy based generative adversarial network is the main proposed model that aims to mitigate the disadvantageous outcomes of stabilization and convergence problems experienced vy the previously mentioned methods (see chapter 2). Even though it is presented incrementally throughout the chapter, its general architecture, training strategy and its approach to anomaly detection problem will be discussed.

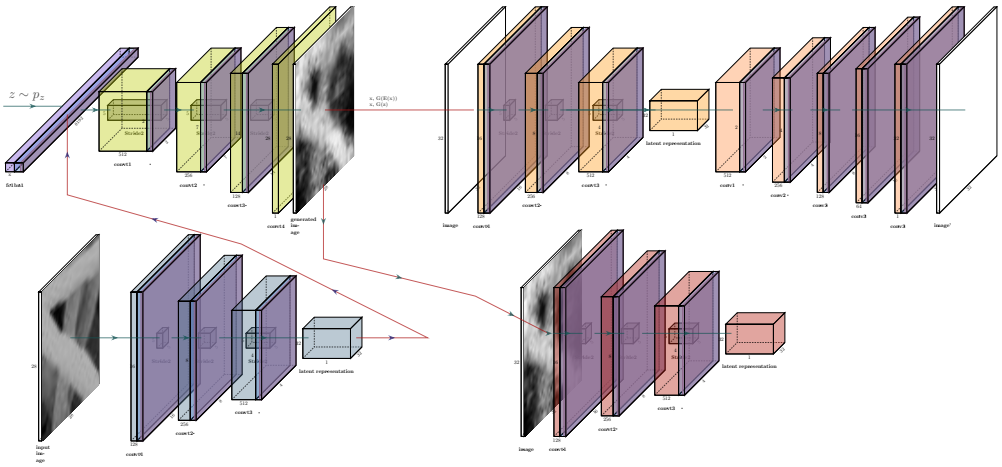

Figure 49 – SENCEBGAN Model Overview

SENCEBGAN model consists of an energy based generative adversarial network and 2 additional encoder networks. The first encoder network learns the representation of training data and its called generator encoder or E_G. Second encoder learns the latent representation of the reconstructions

of the training data provided by the generator network. This encoder network will be mentioned as reconstruction encoder or E_R. Training objective of the model is given in equation 4.5.

$$\begin{aligned} D(x) &= \|\operatorname{Dec}(Enc(x)) - x\| \\ V(G, E_G, E_R, D) &= \underbrace{D(G(z))}_{\text{Generator}} + \underbrace{D(x) + [m - D(G(z))]^+}_{\text{Discriminator}} + \\ &\quad \underbrace{D(G(E_G(x)))}_{\text{Encoder}_G} + \underbrace{\|E_G(x) - E_R(G(E_G(x)))\|^2}_{\text{Encoder}_R} \end{aligned} \tag{4.5}$$

Training objective is divided into three separate sequences. In the first stage of the training, energy based gan framework is trained. After the training is completed, autoencoder architecture is formed by merging E_G and Generator G with fixed weights. Combined with discriminator (also fixed weights) E_G is trained using the reconstruction error produced from the temporary autoencoder configuration. In the last stage, E_R is trained to learn the latent representation of the reconstructed samples. Training is performed using the ℓ_2 norm of the encoded representation residual (see eqn. 4.6).

$$\begin{aligned} \mathcal{L}_{E_G}(x) &= D(G(E(x))) \\ \mathcal{L}_{E_R}(x) &= \|E_G(x) - E_R(G(E_G))(x)\|^2 \end{aligned} \tag{4.6}$$

SENCEBGAN model separates anomaly detection computation into image based and latent dimension based categories. Different anomaly score computations are tested to measure the impact of the additional encoder networks and observe both implicit encoding and reconstruction capability of the discriminator network.

$$\begin{aligned} \mathcal{A}_R(x) &= \|x - G(E_G(x))\|^2 \\ \mathcal{A}_{R_D}(x) &= \|D(x) - D(G(E_G(x)))\|^2 \\ \mathcal{A}_{IC}(x) &= \lambda \cdot \mathcal{A}_R(x) + (1 - \lambda) \cdot \mathcal{A}_{R_D} \end{aligned} \tag{4.7}$$

Score functions defined in equation 4.7 defines the anomaly measure using spatial data. $\mathcal{A}_R(x)$ calculates the reconstruction error during the inference stage. This anomaly score is the one used in all pure GAN based models. In order to test the reconstruction capability of the discriminator $\mathcal{A}_{R_D}(x)$ score is employed. This score is calculated by performing 2 consecutive reconstructions on the sample image. $\mathcal{A}_{IC}(x)$ is image based com-

bination anomaly score implemented to measure each of the image based anomaly scores' affect on an ensemble approach.

$$\begin{aligned} \mathcal{A}_L(x) &= \|E_G(x) - E_R(G(E_G(x)))\|^2 \\ \mathcal{A}_{L_D}(x) &= \left\|E_G(x) - L_{D_Z}(G(E_G(x)))\right\|^2 \\ \mathcal{A}_{L_{D_Z}}(x) &= \left\|L_{D_Z}(x) - L_{D_Z}(G(E_G(x)))\right\|^2 \\ \mathcal{A}_{LC}(x) &= \lambda \cdot \mathcal{A}_L + (1-\lambda) \cdot \mathcal{A}_{L_{D_Z}} \end{aligned} \tag{4.8}$$

Secondary encoder network E_R added to the model's pipeline enabled model to capability to inspect the normality of query images in latent dimensional space and provided an alternative medium regards to anomaly score computation. Inspired by the GANomaly model's (see sec. 2.3.4) evaluation method, various types of anomaly score evaluations based on the latent representation space is depicted in equation 4.8. $\mathcal{A}_L(x)$ measures anomaly score based on the ℓ_2 norm of the difference between encodings obtained during the pipeline. Encoding capability of the discriminator network is also explored in these category. $\mathcal{A}_{L_D}(x)$ and $\mathcal{A}_{L_{D_Z}}(x)$ scores tests the anomaly score by comparing the latent representation obtained by the discriminator network. Finally, combined anomaly score for latent represenation is employed to measure the affect of each score to an ensemble methods.

In terms of the performance, proposed model performed better than all previously mentioned models except GANomaly. Performance analysis and observations regarding to its potential improvements and different configurations will be explored in chapter 5.

CHAPTER 5

Experimental Results

This chapter presents the performance of the gan based anomaly detection models and proposed model.

5.1 Experiment Settings

5.1.1 Performance Metrics

This section will introduce the performance metrics used for the interpretation of the experiments performed. These are:

- Precision
- Recall
- F1 Score
- AUROC (Area Under Receiver Operating Characteristic curve)

Recall is the ability of a model to find all the relevant cases within a dataset. In our case detection of all anomalies in a test would give us a recall of 1.0. **Precision** on the other hand is the ability ofa classification model to identify **only** the relevant data points. While recall expresses the ability to find all relevant instances in a dataset, precision expresses the proportion of the data points our model says was relevant actually were relevant. The calculation of the both metrics is given below

$$\textbf{recall} = \frac{\text{true positives}}{\text{true positives} + \text{false negatives}} \tag{5.1}$$

$$\textbf{precision} = \frac{\text{true positives}}{\text{true positives} + \text{false positives}} \tag{5.2}$$

Precision and recall comprises a trade off situation. If the model favors the precision, the recall decreases because eliminating the false positives inadvertently increases the false negative rate and vice versa. To give equal importance to both metrics, **F1 score** is used. The F1 score is the harmonic mean of precision and recall taking both metrics into account in the following equation:

$$\mathrm{F}_1 = 2 \times \frac{\text{precision} \times \text{recall}}{\text{precision} + \text{recall}} \tag{5.3}$$

The last metric we use to interpret the model performance is area under receiver operating characteristic curve, **AUROC** for short. ROC curve visualizes the trade of relationship between the false positive and true positive rate. True positive rate is actually recall. False positive rate is the probability of false detection for the system. The calculations for these rates are provided below:

$$\textbf{True Positive Rate} = \frac{\text{true positives}}{\text{true positives} + \text{false negatives}} \tag{5.4}$$

$$\textbf{False Positive Rate} = \frac{\text{false positives}}{\text{true negatives} + \text{false positives}} \tag{5.5}$$

the AUROC value can be obtained by calculating the area under the ROC curve which has a range between 0 and 1 with a higher number indicating better classification performance.

5.2 Pure GAN Model Analysis

This section presents the experiment results for the GAN based approaches which

test

5.3 Autoencoder Variant Model Analysis

5.4 Improved Model Analysis

5.5 Discussion of Experiment Results

This chapter will explain the experimental results for all the models and improvements. It will also point out a discussion about what could be

Table 51
Ablation study for AnoGAN to test the effect of various training improvements for stabilization.

Model		Metrics			
		AUROC	Precision	Recall	F1 Score
AnoGAN	Normal				
	IN				
	SL				
	LF				
	IN + SL				
	IN + LF				
	SL + LF				
	LF + SL + IN				

Table 52
Ablation study for BiGAN to test the effect of various training improvements for stabilization.

Model		Metrics			
		AUROC	Precision	Recall	F1 Score
BiGAN	Normal	0.39614			
	IN	0.59329			
	SL	0.54633			
	LF	0.63394			
	IN + SL	0.53644			
	IN + LF	0.54526			
	SL + LF	0.57391			
	LF + SL + IN	0.36905			

improved and the future direction.

There will be 3 classes of models to be considered.

- Models that maps z to x to find the image distrbituion and uses inverse sample for reconstruction → AnoGAN, BiGAN and ALAD
- Models that maps directly image distribution by integrating an encoder to the generator module hence creating in practise an autoencoder, and uses again, reconstruction → Ganomaly and skip ganomaly
- Models that tries new methods to explore different solution strategies
  - Training with full image → Segmentation papers
  - Ganomaly + Noise addition (one Class paper concurrent work)

Table 53
Ablation study for ALAD to test the effect of various training improvements for stabilization.

Model		Metrics			
		AUROC	Precision	Recall	F1 Score
ALAD	Normal				
	IN				
	SL				
	LF				
	IN + SL				
	IN + LF				
	SL + LF				
	LF + SL + IN				

Table 54
Ablation study for GANomaly to test the effect of various training improvements for stabilization.

Model		Metrics			
		AUROC	Precision	Recall	F1 Score
GANomaly	Normal				
	IN				
	SL				
	LF				
	IN + SL				
	IN + LF				
	SL + LF				
	LF + SL + IN				

to improve the performance of the image distribution learning.
  - Energy Based GANS (loss function change), Can this method be applied to the encoder network as well, to better capture the noise distribution.

- All models will be tested with the standard improvements of the gan training.
  - Label Flipping → improves gradints of the discriminator
  - Soft Labels → Better than 0,1 reference the papers
  - Adding noise to the input image and rectrated image to confuse discriminator → robustness

Table 55
Ablation study for Skip-GANomaly to test the effect of various training improvements for stabilization.

Model		**Metrics**			
		AUROC	Precision	Recall	F1 Score
Skip-GANomaly	Normal				
	IN				
	SL				
	LF				
	IN + SL				
	IN + LF				
	SL + LF				
	LF + SL + IN				

- Best performance models then will be tested with a training with validation that is based on the reconstruction of the image.
- All model results with ablation study
- Improved model results
- Visual Results like precision recall, AUC curve, Histogram of Anomalies
- Numerical Results like the result of the model performances in a table '†'

CHAPTER 6

Conclusion and Future Work

This chapter will explain the purpose of the thesis once more and give information about the general process and the result interpretation (1 page)

It will make suggestions based on the improved model experiments and leave an open door for the improvement.

APPENDIX A

Model Implementation Details

This section contains all the model implementation details. The repository for the thesis can be found at this address. All the experiments are conducted with the corresponding configuration files in the **configs** folder. Tensorflow 1.13[1] is used as the underlying framework with Python 3.7[2]

A.1 AnoGAN Implementation

TABLE A1
ARCHITECTURE AND HYPERPARAMETERS OF ANOGAN MODEL

Operation	Kernel	Stride	Feature Maps/ Units	BN ?	Activation
Generator					
Dense			$4 \times 4 \times 512$	✓	Leaky Relu
Transposed Convolution	4×4	2×2	512	✓	Leaky Relu
Transposed Convolution	4×4	2×2	256	✓	Leaky Relu
Transposed Convolution	4×4	2×2	128	✓	Leaky Relu
Transposed Convolution	5×5	1×1	1		TanH
Latent Dimension	256				
Leaky Relu Slope	0.2				
Batch Norm Momentum	0.8				
Optimizer	Adam ($\mathrm{lr} = 5e-5,$ beta $1 = 0.5,$ beta $2 = 0.999,$)				
Discriminator					
Convolution	4×4	2×2	64	✓	Leaky Relu
Convolution	4×4	2×2	128	✓	Leaky Relu
Convolution	4×4	2×2	256	✓	Leaky Relu

[1] https://www.tensorflow.org
[2] https://www.python.org/downloads/release/python-370/

Operation	Kernel	Stride	Feature Maps/ Units	BN ?	Activation
Dense			1		Sigmoid
Leaky ReLU Slope	0.2				
Batch Norm Momentum	0.8				
Optimizer	Adam ($\mathrm{lr} = 1\mathrm{e}-6,$ beta $1 = 0.5,$ beta $2 = 0.999,$)				
Epochs	50				
Batch Size	64				

A.2 BiGAN Implementation

Table A2
Architecture and Hyperparameters of BiGAN Model

Operation	Kernel	Stride	Feature Maps/ Units	BN ?	Activation
Generator					
Dense			$4 \times 4 \times 512$	✓	Leaky Relu
Transposed Convolution	4×4	2×2	512	✓	Leaky Relu
Transposed Convolution	4×4	2×2	256	✓	Leaky Relu
Transposed Convolution	4×4	2×2	128	✓	Leaky Relu
Transposed Convolution	×5	1×1	1		TanH
Latent Dimension	256				
Leaky Relu Slope	0.2				
Batch Norm Momentum	0.8				
Optimizer	Adam ($\mathrm{lr} = 5\mathrm{e}-5,$ beta $1 = 0.5,$ beta $2 = 0.999,$)				
Discriminator					
Convolution	4×4	2×2	64	✓	Leaky Relu
Convolution	4×4	2×2	128	✓	Leaky Relu
Convolution	4×4	2×2	256	✓	Leaky Relu
Dense			1		Sigmoid
Leaky ReLU Slope	0.2				
Batch Norm Momentum	0.8				
Optimizer	Adam ($\mathrm{lr} = 1\mathrm{e}-6,$ beta $1 = 0.5,$ beta $2 = 0.999,$)				
Encoder					
Convolution	4×4	2×2	64		Leaky Relu
Convolution	4×4	2×2	128	✓	Leaky Relu
Convolution	4×4	2×2	256	✓	Leaky Relu
Dense			256		
Leaky ReLU Slope	0.2				
Batch Norm Momentum	0.8				
Optimizer	Adam ($\mathrm{lr} = 1\mathrm{e}-6,$ beta $1 = 0.5,$ beta $2 = 0.999,$)				
Epochs	50				
Batch Size	64				

A.3 ALAD Implementation

TABLE A3
ARCHITECTURE AND HYPERPARAMETERS OF ALAD MODEL

Operation	Kernel	Stride	Feature Maps/ Units	BN ?	Activation
Generator					
Dense			$4 \times 4 \times 512$	✓	Leaky Relu
Transposed Convolution	4×4	2×2	512	✓	Leaky Relu
Transposed Convolution	4×4	2×2	256	✓	Leaky Relu
Transposed Convolution	4×4	2×2	128	✓	Leaky Relu
Transposed Convolution	4×4	1×1	1		TanH
Latent Dimension	256				
Leaky Relu Slope	0.2				
Batch Norm Momentum	0.8				
Optimizer	Adam ($\mathrm{lr} = 5\mathrm{e}-5,\ \mathrm{beta}\ 1 = 0.5,\ \mathrm{beta}\ 2 = 0.999,$)				
Discriminator XZ					
Convolution(x)	4×4	2×2	128	✓	Leaky Relu
Convolution(x)	4×4	2×2	256	✓	Leaky Relu
Convolution(x)	4×4	2×2	512	✓	Leaky Relu
Reshape	Batch $\times 512 \times 4 \times 4$				
Convolution(z)	4×4	2×2	512	Dropout	Leaky Relu
Convolution(z)	4×4	2×2	512	Dropout	Leaky Relu
Concatenate					
Convolution	1×1	1×1	1024	Dropout	Leaky Relu
Convolution	1×1	1×1	1024	Dropout	Leaky Relu
Dense			1		Sigmoid
Leaky ReLU Slope	0.2				
Dropout Rate	0.2				
Batch Norm Momentum	0.8				
Optimizer	Adam ($\mathrm{lr} = 1\mathrm{e}-6,\ \mathrm{beta}\ 1 = 0.5,\ \mathrm{beta}\ 2 = 0.999,$)				
Encoder					
Convolution	4×4	2×2	32	✓	Leaky Relu
Convolution	4×4	2×2	64	✓	Leaky Relu
Convolution	4×4	2×2	128	✓	Leaky Relu
Convolution	4×4	2×2	256	✓	Leaky Relu
Convolution	4×4	2×2	256		
Leaky ReLU Slope	0.2				
Batch Norm Momentum	0.8				
Optimizer	Adam ($\mathrm{lr} = 1\mathrm{e}-6,\ \mathrm{beta}\ 1 = 0.5,\ \mathrm{beta}\ 2 = 0.999,$)				
Discriminator XX					
Concatenate	f				
Convolution	4×4	2×2	64	Dropout	Leaky Relu
Convolution	4×4	2×2	128	Dropout	Leaky Relu
Dense			1		Sigmoid
Leaky ReLU Slope	0.2				
Batch Norm Momentum	0.8				
Optimizer	Adam ($\mathrm{lr} = 1\mathrm{e}-6,\ \mathrm{beta}\ 1 = 0.5,\ \mathrm{beta}\ 2 = 0.999,$)				
Discriminator ZZ					
Dense	4×4	2×2	64	Dropout	Leaky Relu

Operation	Kernel	Stride	Feature Maps/ Units	BN ?	Activation
Dense	4×4	2×2	32	Dropout	Leaky Relu
Dense	4×4	2×2	1	Dropout	Leaky Relu
Leaky ReLU Slope	0.2				
Dropout Rate	0.2				
Batch Norm Momentum	0.8				
Optimizer	Adam ($\mathrm{lr} = 1\mathrm{e}-6,\ \mathrm{beta}\ 1 = 0.5,\ \mathrm{beta}\ 2 = 0.999,$)				
Epochs	50				
Batch Size	64				

A.4 GANomaly Implementation

Table A4
Architecture and Hyperparameters of GANomaly Model

Operation	Kernel	Stride	Feature Maps/ Units	BN ?	Activation
Generator					
Encoder					
Convolution	5×5	2×2	64		Leaky Relu
Convolution	5×5	2×2	128	✓	Leaky Relu
Convolution	5×5	2×2	256	✓	Leaky Relu
Dense			256		
Decoder					
Transposed Convolution	4×4	2×2	256	✓	Leaky Relu
Transposed Convolution	4×4	2×2	128	✓	Leaky Relu
Transposed Convolution	4×4	2×2	64	✓	Leaky Relu
Transposed Convolution	4×4	2×2	32	✓	Leaky Relu
Transposed Convolution	4×4	2×2	16	✓	Leaky Relu
Transposed Convolution	4×4	1×1	1		TanH
Latent Dimension	256				
Leaky Relu Slope	0.2				
Batch Norm Momentum	0.8				
Optimizer	Adam ($\mathrm{lr} = 5\mathrm{e}-5,\ \mathrm{beta}\ 1 = 0.5,\ \mathrm{beta}\ 2 = 0.999,$)				
Encoder 2					
Convolution	5×5	2×2	64		Leaky Relu
Convolution	5×5	2×2	128	✓	Leaky Relu
Convolution	5×5	2×2	256	✓	Leaky Relu
Dense			256		
Discriminator					
Convolution	4×4	2×2	64	✓	Leaky Relu
Convolution	4×4	2×2	128	✓	Leaky Relu
Convolution	4×4	2×2	256	✓	Leaky Relu
Dense			1		Sigmoid
Leaky ReLU Slope	0.2				
Batch Norm Momentum	0.8				
Optimizer	Adam ($\mathrm{lr} = 1\mathrm{e}-6,\ \mathrm{beta}\ 1 = 0.5,\ \mathrm{beta}\ 2 = 0.999,$)				

Operation	Kernel	Stride	Feature Maps/ Units	BN ?	Activation
Epochs	50				
Batch Size	64				

A.5 Skip-GANomaly Implementation

Table A5
Architecture and Hyperparameters of Skip-GANomaly Model

Operation	Kernel	Stride	Feature Maps/ Units	BN ?	Activation
Generator					
Convolution	5×5	2×2	64	✓	Leaky Relu
Convolution	5×5	2×2	128	✓	Leaky Relu
Convolution	5×5	2×2	256	✓	Leaky Relu
Convolution	5×5	2×2	512	✓	Leaky Relu
Convolution	5×5	2×2	512	✓	Leaky Relu
Transposed Convolution	5×5	2×2	512	✓	Leaky Relu
Transposed Convolution	5×5	2×2	256	✓	Leaky Relu
Transposed Convolution	5×5	2×2	128	✓	Leaky Relu
Transposed Convolution	5×5	2×2	64	✓	Leaky Relu
Transposed Convolution	5×5	2×2	1		
Latent Dimension	256				
Leaky Relu Slope	0.2				
Batch Norm Momentum	0.8				
Optimizer	Adam ($\mathrm{lr} = 5\mathrm{e}-5,$ beta $1 = 0.5,$ beta $2 = 0.999,$)				
Discriminator					
Convolution	5×5	2×2	64	✓	Leaky Relu
Convolution	5×5	2×2	128	✓	Leaky Relu
Convolution	5×5	2×2	256	✓	Leaky Relu
Dense			1		Sigmoid
Leaky ReLU Slope	0.2				
Batch Norm Momentum	0.8				
Optimizer	Adam ($\mathrm{lr} = 1\mathrm{e}-6,$ beta $1 = 0.5,$ beta $2 = 0.999,$)				
Epochs	50				
Batch Size	64				

A.6 ENCEBGAN Implementation

Table A6
Architecture and Hyperparameters of ENCEBGAN Model

Operation	Kernel	Stride	Feature Maps/ Units	BN ?	Activation
Generator					

Operation	Kernel	Stride	Feature Maps/ Units	BN ?	Activation
Dense			$4 \times 4 \times 256$	✓	Leaky Relu
Transposed Convolution	5×5	2×2	128	✓	Leaky Relu
Transposed Convolution	5×5	2×2	64	✓	Leaky Relu
Transposed Convolution	5×5	2×2	32	✓	Leaky Relu
Transposed Convolution	5×5	2×2	1		TanH
Latent Dimension	256				
Leaky Relu Slope	0.2				
Batch Norm Momentum	0.8				
Optimizer	Adam ($\mathrm{lr} = 1\mathrm{e}-5,\ \mathrm{beta}\ 1 = 0.5,\ \mathrm{beta}\ 2 = 0.999,$)				
Discriminator					
Convolution	5×5	2×2	32	✓	Leaky Relu
Convolution	5×5	2×2	64	✓	Leaky Relu
Convolution	5×5	2×2	128	✓	Leaky Relu
Dense			256		
Transposed Convolution	5×5	2×2	256	✓	Leaky Relu
Transposed Convolution	5×5	2×2	128	✓	Leaky Relu
Transposed Convolution	5×5	2×2	64	✓	Leaky Relu
Transposed Convolution	5×5	2×2	32	✓	Leaky Relu
Transposed Convolution	5×5	2×2	1		TanH
Latent Dimension	256				
Leaky Relu Slope	0.2				
Batch Norm Momentum	0.8				
Optimizer	Adam ($\mathrm{lr} = 5\mathrm{e}-6,\ \mathrm{beta}\ 1 = 0.5,\ \mathrm{beta}\ 2 = 0.999,$)				
Encoder					
Convolution	5×5	2×2	64		Leaky Relu
Convolution	5×5	2×2	128	✓	Leaky Relu
Convolution	5×5	2×2	256	✓	Leaky Relu
Dense			256		
Leaky ReLU Slope	0.2				
Batch Norm Momentum	0.8				
Optimizer	Adam ($\mathrm{lr} = 5\mathrm{e}-5,\ \mathrm{beta}\ 1 = 0.5,\ \mathrm{beta}\ 2 = 0.999,$)				
Epochs	50				
Batch Size	64				

A.7 SENCEBGAN Implementation

Table A7
Architecture and Hyperparameters of SENCEBGAN Model

Operation	Kernel	Stride	Feature Maps/ Units	BN ?	Activation
Generator					
Dense			$4 \times 4 \times 256$	✓	Leaky Relu
Transposed Convolution	5×5	2×2	128	✓	Leaky Relu
Transposed Convolution	5×5	2×2	64	✓	Leaky Relu
Transposed Convolution	5×5	2×2	32	✓	Leaky Relu

Operation	Kernel	Stride	Feature Maps/ Units	BN ?	Activation
Transposed Convolution	5×5	2×2	1		TanH
Latent Dimension	256				
Leaky Relu Slope	0.2				
Batch Norm Momentum	0.8				
Optimizer	Adam ($\mathrm{lr} = 1\mathrm{e}-5$, beta $1 = 0.5$, beta $2 = 0.999$,)				
Discriminator					
Convolution	5×5	2×2	32	✓	Leaky Relu
Convolution	5×5	2×2	64	✓	Leaky Relu
Convolution	5×5	2×2	128	✓	Leaky Relu
Dense			256		
Transposed Convolution	5×5	2×2	256	✓	Leaky Relu
Transposed Convolution	5×5	2×2	128	✓	Leaky Relu
Transposed Convolution	5×5	2×2	64	✓	Leaky Relu
Transposed Convolution	5×5	2×2	32	✓	Leaky Relu
Transposed Convolution	5×5	2×2	1		TanH
Latent Dimension	256				
Leaky Relu Slope	0.2				
Batch Norm Momentum	0.8				
Optimizer	Adam ($\mathrm{lr} = 5\mathrm{e}-6$, beta $1 = 0.5$, beta $2 = 0.999$,)				
Encoder					
Convolution	5×5	2×2	64		Leaky Relu
Convolution	5×5	2×2	128	✓	Leaky Relu
Convolution	5×5	2×2	256	✓	Leaky Relu
Dense			256		
Leaky ReLU Slope	0.2				
Batch Norm Momentum	0.8				
Optimizer	Adam ($\mathrm{lr} = 5\mathrm{e}-5$, beta $1 = 0.5$, beta $2 = 0.999$,)				
Encoder 2					
Convolution	5×5	2×2	64		Leaky Relu
Convolution	5×5	2×2	128	✓	Leaky Relu
Convolution	5×5	2×2	256	✓	Leaky Relu
Dense			256		
Leaky ReLU Slope	0.2				
Batch Norm Momentum	0.8				
Optimizer	Adam ($\mathrm{lr} = 5\mathrm{e}-5$, beta $1 = 0.5$, beta $2 = 0.999$,)				
Discriminator XX					
Concatenate	f				
Convolution	4×4	2×2	64	Dropout	Leaky Relu
Convolution	4×4	2×2	128	Dropout	Leaky Relu
Dense			1		Sigmoid
Leaky ReLU Slope	0.2				
Batch Norm Momentum	0.8				
Optimizer	Adam ($\mathrm{lr} = 1\mathrm{e}-6$, beta $1 = 0.5$, beta $2 = 0.999$,)				
Discriminator ZZ					
Dense	4×4	2×2	64	Dropout	Leaky Relu
Dense	4×4	2×2	32	Dropout	Leaky Relu

Operation	Kernel	Stride	Feature Maps/ Units	BN ?	Activation
Dense	4×4	2×2	1	Dropout	Leaky Relu
Leaky ReLU Slope	0.2				
Dropout Rate	0.2				
Batch Norm Momentum	0.8				
Optimizer	Adam ($\mathrm{lr} = 1\mathrm{e}-6,$ beta $1 = 0.5,$ beta $2 = 0.999,$)				
Epochs	50				
Batch Size	64				

Bibliography

[1] Mohiuddin Ahmed, Abdun Naser Mahmood, and Jiankun Hu. "A survey of network anomaly detection techniques". In: *Journal of Network and Computer Applications* 60 (2016), pp. 19 –31. ISSN: 1084-8045. DOI: https://doi.org/10.1016/j.jnca.2015.11.016. URL: http://www.sciencedirect.com/science/article/pii/S1084804515002891.

[2] Samet Akçay, Amir Atapour Abarghouei, and Toby P. Breckon. "GANomaly: Semi-supervised Anomaly Detection via Adversarial Training". In: *ACCV*. 2018.

[3] Samet Akçay, Amir Atapour Abarghouei, and Toby P. Breckon. "Skip-GANomaly: Skip Connected and Adversarially Trained Encoder-Decoder Anomaly Detection". In: *CoRR* abs/1901.08954 (2019).

[4] Jinwon An and Sungzoon Cho. "Variational autoencoder based anomaly detection using reconstruction probability". In: *Special Lecture on IE* 2 (2015), pp. 1–18.

[5] Plamen Angelov, Ramin Ramezani, and Xiaowei Zhou. "Autonomous Novelty Detection and Object Tracking in Video Streams using Evolving Clustering and Takagi-Sugeno type Neuro-Fuzzy System". In: June 2008, pp. 1456–1463. DOI: 10.1109/IJCNN.2008.4633989.

[6] Martin Arjovsky and Léon Bottou. "Towards Principled Methods for Training Generative Adversarial Networks". In: *stat* 1050 (Jan. 2017).

[7] Martín Arjovsky, Soumith Chintala, and Léon Bottou. "Wasserstein GAN". In: *CoRR* abs/1701.07875 (2017).

[8] M. Behniafar, A.R. Nowroozi, and H.R. Shahriari. "A Survey of Anomaly Detection Approaches in Internet of Things". In: *The ISC International Journal of Information Security* 10.2 (2018), pp. 79–92. ISSN: 2008-2045. DOI: 10.22042/isecure.2018.116976.408. eprint: http://www.isecure-journal.com/article___835f5ca77e495cec328b957653e1f4d566995.pdf. URL: http://www.isecure-journal.com/article_66995.html.

[9] Yoshua Bengio. "Learning Deep Architectures for AI". In: *Found. Trends Mach. Learn.* 2.1 (Jan. 2009), pp. 1–127. ISSN: 1935-8237. DOI: 10.1561/2200000006. URL: http://dx.doi.org/10.1561/2200000006.

[10] Patrick Billingsley. *Probability and Measure*. Second. John Wiley and Sons, 1986.

[11] Giacomo Boracchi, Diego Carrera, and Brendt Wohlberg. "Novelty detection in images by sparse representations". In: *2014 IEEE Symposium on Intelligent Embedded Systems (IES)*. IEEE. 2014, pp. 47–54.

[12] Diego Carrera et al. "Defect detection in SEM images of nanofibrous materials". In: *IEEE Transactions on Industrial Informatics* 13.2 (2016), pp. 551–561.

[13] Diego Carrera et al. "Scale-invariant anomaly detection with multiscale group-sparse models". In: *Proceedings of IEEE International Conference on Image Processing (ICIP)*. Phoenix, AZ, USA, Sept. 2016, pp. 3892–3896. DOI: 10.1109/ICIP.2016.7533089.

[14] Varun Chandola, Arindam Banerjee, and Vipin Kumar. "Anomaly Detection: A Survey". In: *ACM Comput. Surv.* 41.3 (July 2009), 15:1–15:58. ISSN: 0360-0300. DOI: 10.1145/1541880.1541882. URL: http://doi.acm.org/10.1145/1541880.1541882.

[15] Lei Clifton et al. "Identification of Patient Deterioration in Vital-Sign Data using One-Class Support Vector Machines." In: Jan. 2011, pp. 125–131.

[16] Thomas M. Cover and Joy A. Thomas. *Elements of Information Theory (Wiley Series in Telecommunications and Signal Processing)*. New York, NY, USA: Wiley-Interscience, 2006. ISBN: 0471241954.

[17] Jeff Donahue, Philipp Krähenbühl, and Trevor Darrell. "Adversarial Feature Learning". In: *CoRR* abs/1605.09782 (2017).

[18] Vincent Dumoulin et al. "Adversarially Learned Inference". In: *CoRR* abs/1606.00704 (2017).

[19] Gilberto Fernandes et al. "Network anomaly detection using IP flows with Principal Component Analysis and Ant Colony Optimization". In: *Journal of Network and Computer Applications* 64 (2016), pp. 1 –11. ISSN: 1084-8045. DOI: https://doi.org/10.1016/j.jnca.2015.11.024. URL: http://www.sciencedirect.com/science/article/pii/S1084804516000618.

[20] Ugo Fiore et al. “Using Generative Adversarial Networks for Improving Classification Effectiveness in Credit Card Fraud Detection”. In: *Information Sciences* (Dec. 2017). DOI: 10.1016/j.ins.2017.12.030.

[21] Xavier Glorot, Antoine Bordes, and Yoshua Bengio. “Deep Sparse Rectifier Neural Networks”. In: *AISTATS*. 2011.

[22] Ian Goodfellow, Yoshua Bengio, and Aaron Courville. *Deep Learning*. http://www.deeplearningbook.org. MIT Press, 2016.

[23] Ian J. Goodfellow et al. “Generative Adversarial Nets”. In: *Proceedings of the 27th International Conference on Neural Information Processing Systems - Volume 2*. NIPS’14. Montreal, Canada: MIT Press, 2014, pp. 2672–2680. URL: http://dl.acm.org/citation.cfm?id=2969033.2969125.

[24] Ishaan Gulrajani et al. “Improved Training of Wasserstein GANs”. In: *NIPS*. 2017.

[25] Kaiming He et al. “Deep residual learning for image recognition”. In: *Proceedings of the IEEE conference on computer vision and pattern recognition*. 2016, pp. 770–778.

[26] Phillip Isola et al. “Image-to-Image Translation with Conditional Adversarial Networks”. In: *2017 IEEE Conference on Computer Vision and Pattern Recognition (CVPR)* (2017), pp. 5967–5976.

[27] J. Jabez and B. Muthukumar. “Intrusion Detection System (IDS): Anomaly Detection Using Outlier Detection Approach”. In: *Procedia Computer Science* 48 (2015). International Conference on Computer, Communication and Convergence (ICCC 2015), pp. 338 –346. ISSN: 1877-0509. DOI: https://doi.org/10.1016/j.procs.2015.04.191. URL: http://www.sciencedirect.com/science/article/pii/S1877050915007000.

[28] Dongil Kim et al. “Machine Learning-based Novelty Detection for Faulty Wafer Detection in Semiconductor Manufacturing”. In: *Expert Syst. Appl.* 39.4 (Mar. 2012), pp. 4075–4083. ISSN: 0957-4174. DOI: 10.1016/j.eswa.2011.09.088. URL: http://dx.doi.org/10.1016/j.eswa.2011.09.088.

[29] Taeksoo Kim et al. “Learning to Discover Cross-Domain Relations with Generative Adversarial Networks”. In: *ICML*. 2017.

[30] Walter Kramer. "Probability & Measure : Patrick Billingsley (1995): (3rd ed.). New York : Wiley, ISBN 0-471-0071-02, pp 593, [pound sign] 49.95". In: *Computational Statistics & Data Analysis* 20.6 (1995), pp. 702–703. URL: https://ideas.repec.org/a/eee/csdana/v20y1995i6p703-702.html.

[31] Alex Krizhevsky, Vinod Nair, and Geoffrey Hinton. "CIFAR-10 (Canadian Institute for Advanced Research)". In: (). URL: http://www.cs.toronto.edu/~kriz/cifar.html.

[32] Anders Boesen Lindbo Larsen et al. "Autoencoding beyond pixels using a learned similarity metric". In: *ICML*. 2016.

[33] Yann LeCun et al. "A tutorial on energy-based learning". In: *PREDICTING STRUCTURED DATA*. MIT Press, 2006.

[34] Valentin Leveau and Alexis Joly. "Adversarial autoencoders for novelty detection". In: (2017).

[35] Chunyuan Li et al. "Towards Understanding Adversarial Learning for Joint Distribution Matching". In: *NIPS*. 2017.

[36] Markos Markou and Sameer Singh. "Novelty Detection: A Review&Mdash;Part 2: Neural Network Based Approaches". In: *Signal Process.* 83.12 (Dec. 2003), pp. 2499–2521. ISSN: 0165-1684. DOI: 10.1016/j.sigpro.2003.07.019. URL: http://dx.doi.org/10.1016/j.sigpro.2003.07.019.

[37] Luis Martí et al. "Anomaly Detection Based on Sensor Data in Petroleum Industry Applications". In: *Sensors* 15.2 (2015), pp. 2774–2797. ISSN: 1424-8220. DOI: 10.3390/s150202774. URL: http://www.mdpi.com/1424-8220/15/2/2774.

[38] Takeru Miyato et al. "Spectral Normalization for Generative Adversarial Networks". In: Feb. 2018.

[39] Paolo Napoletano, Flavio Piccoli, and Raimondo Schettini. "Anomaly Detection in Nanofibrous Materials by CNN-Based Self-Similarity". In: *Sensors* 18.2 (2018), p. 209. ISSN: 1424-8220. DOI: 10.3390/s18010209. URL: http://dx.doi.org/10.3390/s18010209.

[40] Yuval Netzer et al. "Reading Digits in Natural Images with Unsupervised Feature Learning". In: 2011.

[41] Stanislav Pidhorskyi et al. "Generative Probabilistic Novelty Detection with Adversarial Autoencoders". In: *Proceedings of the 32Nd International Conference on Neural Information Processing Systems*. NIPS'18. Montréal, Canada: Curran Associates Inc., 2018, pp. 6823–6834. URL: http://dl.acm.org/citation.cfm?id=3327757.3327787.

[42] Marco A. F. Pimentel et al. “Review: A Review of Novelty Detection”. In: *Signal Process.* 99 (June 2014), pp. 215–249. ISSN: 0165-1684. DOI: 10.1016/j.sigpro.2013.12.026. URL: http://dx.doi.org/10.1016/j.sigpro.2013.12.026.

[43] Alec Radford, Luke Metz, and Soumith Chintala. “Unsupervised Representation Learning with Deep Convolutional Generative Adversarial Networks”. In: *CoRR* abs/1511.06434 (2016).

[44] Bengt Ringnér. “Law of the unconscious statistician”. In: (2009).

[45] George G Roussas. *An introduction to measure-theoretic probability*. Burlington, MA: Elsevier, 2004. URL: http://cds.cern.ch/record/1614120.

[46] Mohammad Sabokrou et al. *Adversarially Learned One-Class Classifier for Novelty Detection*. cite arxiv:1802.09088Comment: CVPR 2018 Accepted Paper. 2018. URL: http://arxiv.org/abs/1802.09088.

[47] Ruslan Salakhutdinov and Geoffrey Hinton. “Deep Boltzmann Machines”. In: *Proceedings of the Twelth International Conference on Artificial Intelligence and Statistics*. Ed. by David van Dyk and Max Welling. Vol. 5. Proceedings of Machine Learning Research. Hilton Clearwater Beach Resort, Clearwater Beach, Florida USA: PMLR, 2009, pp. 448–455. URL: http://proceedings.mlr.press/v5/salakhutdinov09a.html.

[48] Tim Salimans et al. “Improved Techniques for Training GANs”. In: (June 2016).

[49] Thomas Schlegl et al. “f-AnoGAN: Fast Unsupervised Anomaly Detection with Generative Adversarial Networks”. In: *Medical Image Analysis* 54.Data Mining and Knowledge Discovery 29 3 2015 (2019), pp. 30–44. DOI: 10.1016/j.media.2019.01.010. URL: https://app.dimensions.ai/details/publication/pub.1111824956.

[50] Thomas Schlegl et al. “Unsupervised Anomaly Detection with Generative Adversarial Networks to Guide Marker Discovery”. In: *IPMI*. 2017.

[51] “SEM Image Dataset)”. In: (). URL: http://web.mi.imati.cnr.it/ettore/NanoTwice.

[52] H.H. Sohrab. *Basic Real Analysis*. Birkhäuser Boston, 2011. ISBN: 9780817682323. URL: https://books.google.it/books?id=zjfaBwAAQBAJ.

[53] Nitish Srivastava et al. “Dropout: a simple way to prevent neural networks from overfitting”. In: *Journal of Machine Learning Research* 15 (2014), pp. 1929–1958.

[54] Raihan Ul Islam, Mohammad Shahadat Hossain, and Karl Andersson. "A novel anomaly detection algorithm for sensor data under uncertainty". In: *Soft Computing* 22.5 (2018), pp. 1623–1639. ISSN: 1433-7479. DOI: 10.1007/s00500-016-2425-2. URL: https://doi.org/10.1007/s00500-016-2425-2.

[55] Bernard Widrow and Eugene Walach. "Appendix G: Thirty Years of Adaptive Neural Networks: Perceptron, Madaline, and Backpropagation". In: 2008.

[56] Zili Yi et al. "DualGAN: Unsupervised Dual Learning for Image-to-Image Translation". In: *2017 IEEE International Conference on Computer Vision (ICCV)* (2017), pp. 2868–2876.

[57] Houssam Zenati et al. "Adversarially Learned Anomaly Detection". In: *CoRR* abs/1812.02288 (2018). arXiv: 1812.02288. URL: http://arxiv.org/abs/1812.02288.

[58] Junbo Jake Zhao, Michaël Mathieu, and Yann LeCun. "Energy-based Generative Adversarial Network". In: *CoRR* abs/1609.03126 (2016).

[59] Jun-Yan Zhu et al. "Unpaired Image-to-Image Translation Using Cycle-Consistent Adversarial Networks". In: *2017 IEEE International Conference on Computer Vision (ICCV)* (2017), pp. 2242–2251.

[60] Maria Zontak and Israel Cohen. "Defect detection in patterned wafers using anisotropic kernels". In: *Machine Vision and Applications* 21.2 (2010), pp. 129–141.